European Journal of Taxonomy 1012: 172–200
https://doi.org/10.5852/ejt.2025.1012.3037

europeanjournaloftaxonomy.eu
ISSN 2118-9773
2025 · Truong X.L. *et al.*

Received: 8 February 2025 • *Accepted: 25 June 2025* • *Published: 4 September 2025*

Topic editor: Tony Robillard • *Section editor: Christopher Dietrich* • *Desk editor: Pepe Fernández*

Research article

urn:lsid:zoobank.org:pub:C5A11EF1-0ECC-4769-AC8D-70348321A1D8

Epidaus batxatensis and *Epidaus konkakinhensis*, two new species of the genus *Epidaus* Stål (Insecta: Hemiptera: Reduviidae: Harpactorinae) from Vietnam

Xuan Lam TRUONG[1], Thi Giang PHAN[2], Thi Ngoc Lam THAI[3], Dai Dac NGUYEN[4] & Ngoc Linh HA[5,*]

[1,4,5]Institute of Biology, Vietnam Academy of Science and Technology, Hanoi, Vietnam, 18 Hoang Quoc Viet Road, Nghia Do, Cau Giay, Hanoi, Vietnam.
[1,2,4]Graduate University of Science and Technology, Vietnam Academy of Science and Technology, 18 Hoang Quoc Viet Road, Nghia Do, Cau Giay, Hanoi, Vietnam.
[2,3]Vinh University, 182 Le Duan, Vinh, Nghe An, Vietnam.

[*]Corresponding author: linh.hangoc02@gmail.com
[1]Email: txlam.iebr@gmail.com
[2]Email: tragiangdhv8668@gmail.com
[3]Email: ngoclamthaidhv@gmail.com
[4]Email: daindiebr@gmail.com

Abstract. The genus *Epidaus* Stål, 1859 includes 26 valid species, distributed widely in the Oriental and Sino-Japanese realms. Among them, four species, *Epidaus bachmaensis* Truong, Zhao & Cai, 2006, *E. famulus* (Stål, 1904), *E. longispinus* Hsiao, 1979, and *E. sexspinus* Hsiao, 1979, were recorded and described from Vietnam. In this study, we conduct the examination of species of the genus *Epidaus* collected from Vietnam based on an integrative taxonomy, including morphological examination, morphometric analyses (Principal Component Analyses), molecular phylogenetic analyses (Bayesian Inference Analyses), and species delimitation analyses (Assemble Species by Automatic Partitioning and Bayesian implementation of the Poisson Tree Processes model). As a result, two new species of the genus *Epidaus* Stål, 1859, i.e., *Epidaus batxatensis* Truong, Nguyen & Ha sp. nov. and *Epidaus konkakinhensis* Truong, Nguyen & Ha sp. nov., are herein discovered and described.

Keywords. Assassin bug, Vietnam, morphometry, molecular phylogeny, taxonomy.

Truong X.L., Phan T.G., Thai T.N.L., Nguyen D.D.& Ha N.L. 2025. *Epidaus batxatensis* and *Epidaus konkakinhensis*, two new species of the genus *Epidaus* Stål (Insecta: Hemiptera: Reduviidae: Harpactorinae) from Vietnam. *European Journal of Taxonomy* 1012: 172–200. https://doi.org/10.5852/ejt.2025.1012.3037

Introduction

Epidaus Stål, 1859 is a genus of the subfamily Harpactorinae Amyot & Serville, 1843 (Hemiptera: Heteroptera: Reduviidae) which was established by heteropterist Carl Stål in 1859 with the type species

Zelus transversus Burmeister, 1835 from the Philippines (Stål 1859) by subsequent designation (Distant 1904). Species of *Epidaus* play an important role in controlling herbivorous insect populations, including forestry and agricultural pests, thereby reducing plant and crop damage (Miller 1956). Like other species of Reduviidae Latreille, 1807, species of *Epidaus* exhibit typical assassin bug traits and are sensitive to environmental changes, making their diversity a useful bioindicator of ecosystem health, particularly in tropical forests (Ambrose 1999). Despite their ecological importance, they remain poorly studied in terms of taxonomy, ecology, life history, and potential use in pest management.

The genus *Epidaus* is mainly distributed in the Oriental and Sino-Japanese regions, with 26 recognized species reported from Vietnam, India, China, Malaysia, and Indonesia (Burmeister 1835; Stål 1859, 1863, 1874; Breddin 1900; Distant 1903, 1904, 1919; Bergroth 1915; Yang 1940; Miller 1941, 1948; Hsiao 1979; Truong *et al*. 2006; Zhang *et al*. 2010; Chen *et al*. 2016; Truong 2019). However, many areas remain unsurveyed, and further taxon sampling is needed to better understand the genus's species diversity, ecology, and potential in biocontrol.

Of the 26 known species of *Epidaus*, four, *Epidaus famulus* (Stål, 1904), *E. bachmaensis* Truong, Zhao & Cai, 2006, *E. longispinus* Hsiao, 1979, and *E. sexspinus* Hsiao, 1979, have been recorded from Vietnam. Since the addition of *E. bachmaensis* by Truong *et al.* (2006), the classification of *Epidaus* in the region has remained largely unchanged. In our recent examination of hemipteran specimens from the Institute of Biology (IB), two new species of *Epidaus* were discovered and are described here.

Material and methods

Material examined and specimen depository

Specimens of *Epidaus* were gathered by sweeping through the shrubs and vegetation along trails in forested areas, including evergreen and restored forests, in Vietnam.

A total of 41 *Epidaus* adult male (♂) and female (♀) specimens from the Institute of Biology (IB) and a COI sequence of *Epidaus tuberosus* Yang, 1940 obtained from GenBank were analyzed as ingroups (Table 1). Furthermore, a specimen of each of the following species, *Rhynocoris marginellus* (Fabricius, 1803), *Sycanus bifidus* (Fabricius, 1787), and *Velinus rufiventris* Hsiao, 1797 from Vietnam, was involved in the analyses as outgroups (Table 1). The definitions of the genus *Epidaus* used as working hypotheses are given by Chen *et al.* (2016) as follows: body elongated; head slightly shorter than pronotum, with a process behind each antennal insertion; postocular area of head nearly 1.5 times as long as anteocular area; first visible labial segment as long as second and third segments combined; posterior pronotal lobe with a pair of spines or tubercles at middle; lateral angles of pronotum produced to form a sharp spine, each spine with a much smaller tooth-like spine or a tubercle behind; fore femora thicker than mid and hind femora, the latter two nearly similarly thickened.

The voucher specimens of this study are deposited in IB-DEB – Department of Experimental Biocontrol, Institute of Biology, Vietnam Academy of Science and Technology, Vietnam.

Morphological examination of the validly named species of the genus was conducted by referring to the original descriptions, other taxonomic publications, and type specimens where available of the congeners of the genus *Epidaus* known from Vietnam and adjacent areas (Burmeister 1835; Stål 1859, 1863, 1874; Breddin 1900; Distant 1903, 1904, 1919; Bergroth 1915; Yang 1940; Miller 1941, 1948; Hsiao 1979; Truong *et al.* 2006; Zhang *et al.* 2010; Chen *et al.* 2016; Truong 2019).

Specimens were labeled with their specimen identifications and locality information, and individually preserved in vials containing 99% ethanol. The right hind leg or right mid leg of each individual was cut off for DNA extraction (then for molecular phylogenetic analysis and DNA barcoding). The rest of the body was pinned for morphological study.

Table 1 (continued on next two pages). The data on specimens used in this study. Abbreviations and symbols: IB-DEB = Department of Experimental Biocontrol, Institute of Biology, Vietnam Academy of Science and Technology, Vietnam, tentatively held by Ha N.L. (corresponding author); n/a = no data; SNU = Seoul National University.

Morphospecies [clade or singleton lineage in Figs 5–6]	Specimen code	Collecting date	Locality	Sex	Accession numbers COI	Depository
***Epidaus* (ingroups)**						
Epidaus batxatensis Truong, Nguyen & Ha sp. nov. [α] [Holotype]	HNL2024-234	26 Jul. 2024	Vietnam, Lao Cai	♂	PQ142809	IB-DEB
Epidaus batxatensis Truong, Nguyen & Ha sp. nov. [α] [Paratype]	HNL2024-230	26 Jul. 2024	Vietnam, Lao Cai	♂	PQ142810	IB-DEB
Epidaus batxatensis Truong, Nguyen & Ha sp. nov. [α] [Paratype]	HNL2024-231	26 Jul. 2024	Vietnam, Lao Cai	♂	PQ142811	IB-DEB
Epidaus batxatensis Truong, Nguyen & Ha sp. nov. [α] [Paratype]	HNL2024-235	26 Jul. 2024	Vietnam, Lao Cai	♂	PQ142812	IB-DEB
Epidaus batxatensis Truong, Nguyen & Ha sp. nov. [α] [Paratype]	HNL2024-238	26 Jul. 2024	Vietnam, Lao Cai	♀	PQ142813	IB-DEB
Epidaus batxatensis Truong, Nguyen & Ha sp. nov. [α] [Paratype]	HNL2024-239	26 Jul. 2024	Vietnam, Lao Cai	♂	PQ142814	IB-DEB
Epidaus batxatensis Truong, Nguyen & Ha sp. nov. [α] [Paratype]	HNL2024-240	26 Jul. 2024	Vietnam, Lao Cai	♂	PQ142815	IB-DEB
Epidaus batxatensis Truong, Nguyen & Ha sp. nov. [α] [Paratype]	HNL2024-242	26 Jul. 2024	Vietnam, Lao Cai	♂	PQ142816	IB-DEB
Epidaus batxatensis Truong, Nguyen & Ha sp. nov. [α] [Paratype]	HNL2024-243	26 Jul. 2024	Vietnam, Lao Cai	♀	PQ142817	IB-DEB
Epidaus batxatensis Truong, Nguyen & Ha sp. nov. [α] [Paratype]	HNL2024-244	26 Jul. 2024	Vietnam, Lao Cai	♂	PQ142818	IB-DEB
Epidaus batxatensis Truong, Nguyen & Ha sp. nov. [α] [Paratype]	HNL2024-245	26 Jul. 2024	Vietnam, Lao Cai	♂	PQ142819	IB-DEB
Epidaus batxatensis Truong, Nguyen & Ha sp. nov. [α] [Paratype]	HNL2024-272	26 Jul. 2024	Vietnam, Lao Cai	♀	PQ142820	IB-DEB
Epidaus batxatensis Truong, Nguyen & Ha sp. nov. [α] [Paratype]	HNL2024-276	26 Jul. 2024	Vietnam, Lao Cai	♀	PQ142821	IB-DEB
Epidaus batxatensis Truong, Nguyen & Ha sp. nov. [α] [Paratype]	HNL2024-277	26 Jul. 2024	Vietnam, Lao Cai	♀	PQ142822	IB-DEB
Epidaus batxatensis Truong, Nguyen & Ha sp. nov. [α]	HNL2024-229	26 Jul. 2024	Vietnam, Lao Cai	♀	PQ142823	IB-DEB
Epidaus batxatensis Truong, Nguyen & Ha sp. nov. [α]	HNL2024-246	26 Jul. 2024	Vietnam, Lao Cai	♀	PQ142824	IB-DEB

Table 1 (continued). The data on specimens used in this study.

Morphospecies [clade or singleton lineage in Figs 5–6]	Specimen code	Collecting date	Locality	Sex	Accession numbers	Depository
					COI	
Epidaus batxatensis Truong, Nguyen & Ha sp. nov. [α]	HNL2024-247	26 Jul. 2024	Vietnam, Lao Cai	♂	PQ142825	IB-DEB
Epidaus batxatensis Truong, Nguyen & Ha sp. nov. [α]	HNL2024-248	26 Jul. 2024	Vietnam, Lao Cai	♀	PQ142826	IB-DEB
Epidaus batxatensis Truong, Nguyen & Ha sp. nov. [α]	HNL2024-249	26 Jul. 2024	Vietnam, Lao Cai	♂	PQ142827	IB-DEB
Epidaus batxatensis Truong, Nguyen & Ha sp. nov. [α]	HNL2024-262	26 Jul. 2024	Vietnam, Lao Cai	♂	PQ142828	IB-DEB
Epidaus batxatensis Truong, Nguyen & Ha sp. nov. [α]	TXL2024-451	28 Mar. 2024	Vietnam, Lai Chau	♀	PQ142829	IB-DEB
Epidaus batxatensis Truong, Nguyen & Ha sp. nov. [α]	TXL2024-510	1 Apr. 2024	Vietnam, Lai Chau	♀	PQ142830	IB-DEB
Epidaus konkakinhensis Truong, Nguyen & Ha sp. nov. [β] [Holotype]	TXL2022-148	26 Mar. 2022	Vietnam, Gia Lai	♂	PQ142831	IB-DEB
Epidaus konkakinhensis Truong, Nguyen & Ha sp. nov. [β] [Paratype]	TXL2022-149	26 Mar. 2022	Vietnam, Gia Lai	♂	PQ142832	IB-DEB
Epidaus konkakinhensis Truong, Nguyen & Ha sp. nov. [β]	TXLBXN4	26 Mar. 2022	Vietnam, Gia Lai	♂	n/a	IB-DEB
Epidaus konkakinhensis Truong, Nguyen & Ha sp. nov. [β]	TXL2024-156	3 Feb. 2024	Vietnam, Thua Thien Hue	♂	PQ142833	IB-DEB
E. bachmaensis Truong, Zhao & Cai, 2006	TXL2016-591	4 May 2016	Vietnam, Thua Thien Hue	♀	PQ142834	IB-DEB
E. bachmaensis Truong, Zhao & Cai, 2006	TXL2018-053	8 May 2018	Vietnam, Thua Thien Hue	♀	PQ142835	IB-DEB
E. bachmaensis Truong, Zhao & Cai, 2006	TXL2016-001	4 May 2016	Vietnam, Thua Thien Hue	♂	n/a	IB-DEB
E. bachmaensis Truong, Zhao & Cai, 2006	TXL2016-002	4 May 2016	Vietnam, Thua Thien Hue	♂	n/a	IB-DEB
E. famulus (Stål, 1863)	TXL2024-633	10 May 2024	Vietnam, Nghe An	♀	n/a	IB-DEB
E. famulus (Stål, 1863)	TXL2023-034	20 Oct. 2023	Vietnam, Phu Tho	♀	PQ142836	IB-DEB
E. famulus (Stål, 1863)	TXL2023-035	20 Oct. 2023	Vietnam, Phu Tho	♀	PQ142837	IB-DEB
E. famulus (Stål, 1863)	TXL2023-036	20 Oct. 2023	Vietnam, Phu Tho	♂	PQ142838	IB-DEB
E. famulus (Stål, 1863)	NDD2024-010	15 Mar.2024	Vietnam, Gia Lai	♂	n/a	IB-DEB
E. famulus (Stål, 1863)	TXL2021-124	2 Nov. 2021	Vietnam, Cao Bang	♂	n/a	IB-DEB
E. famulus (Stål, 1863)	TXL2021-125	2 Nov. 2021	Vietnam, Cao Bang	♂	n/a	IB-DEB

Table 1 (continued). The data on specimens used in this study.

Morphospecies [clade or singleton lineage in Figs 5–6]	Specimen code	Collecting date	Locality	Sex	Accession numbers COI	Depository
E. longispinus Hsiao, 1979	HNL2024-038	12 May 2024	Vietnam, Cao Bang	♂	PQ142839	IB-DEB
E. longispinus Hsiao, 1979	TXL2023-831	8 Sep. 2023	Vietnam, Vinh Phuc	♀	PQ142840	IB-DEB
E. sexipinus Hsiao, 1979	LiaoH2019-016	22 Jul. 2019	Japan, Okinawa	n/a	PQ142841	IB-DEB
E. sexipinus Hsiao, 1979	LiaoH2019-017	22 Jul. 2019	Japan, Okinawa	n/a	PQ142842	IB-DEB
E. tuberosus Yang, 1940	SNU#HEM248	25 Sep. 2008	Korea, Jeollanam-do	n/a	GQ292196	SNU (Jung *et al.* 2011)
Outgroups						
Sycanus bifidus (Fabricius, 1787)	AD2021-006	10 May 2021	Vietnam, Cao Bang		PP834511	IB-DEB
Velinus rufiventris Hsiao, 1979	DTH2022-002	13 Apr. 2022	Vietnam, Dien Bien		PQ142843	IB-DEB
Rhynocoris marginellus (Fabricius, 1803)	TXLBX15	13 Jun. 2016	Vietnam, Thanh Hoa		PP647803	IB-DEB

Morphological examination and imaging

External morphological characteristics were examined for dry-mounted specimens using a Nikon SMZ1270 stereo microscope. The genitalia were prepared for examination as described below. Firstly, each male specimen was relaxed by soaking for three days in 70% ethanol. After that, the male genitalia was detached from the body and then soaked in hot solution of 10% KOH for five minutes until the body fat and muscle were released. The endosoma was pulled out of the phallosoma by fine tweezers after removing the phallus from the pygophore. All parts of the male genitalia were preserved in a genitalia vial filled with propylene glycol and subsequently associated with the pinned specimens. Next, the female genitalia were inspected without being detached from the body. A Nikon SMZ1270 stereo microscope was used to examine the male and female genital morphology.

Focus stacking was executed using Helicon Focus Pro ver. 8.2.0 software (Khmelik *et al.* 2006) based on a sequence of the source pictures photographed by a Canon EOS Kiss X10 digital camera connected to a Nikon AZ100 stereo microscope, and artifacts were removed using the retouch function of the software. After that, the contrast, brightness, color balance, and intensity were adjusted using Adobe Photoshop Elements ver. 10.0 software (Adobe Systems Incorporated, San Jose, CA, USA) using a color corresponding sticker (CASMATCH, Bear Medic Corporation, Japan).

Morphological terminology, measurement, and indices

Morphological terminology followed that of Rosa *et al.* (2005), Forero & Weirauch (2012), Schuh & Weirauch (2020), Ha *et al.* (2022), and Truong *et al.* (2024), and was illustrated in Figs 1–2. The following parts of the bodies were measured for *Epidaus* samples (Fig. 3), using the software Image-J (http://imageJ.nih.gov/ij/) based on the direct stacking pictures designed as stated above. The assessment features are stated below, and all dimensions are given in mm.

Measurements characters

A1L = length of scape
A2L = length of pedicel

A3L = length of first flagellomere
A4L = length of second flagellomere
AFL = length of left fore femur
AoL = length of anteocular area of head
AoW = width of anteocular area of head, measured immediately in front of compound eyes
APL = length of anterior pronotal lobe
ATL = length of left fore tibia
BL = body length excluding hemelytra
COD = minimum distance between postero-inner margin of left compound eye and antero-outer margin of left lateral ocellus
CPSL = length of central pronotal spine
ED = maximum diameter of left compound eye
HeL = length of right hemelytron
HeW = maximum width of right hemelytron
HL = head length
HSD = minimum distance measured between apex of two lateral head spines
HSL = length of left lateral head spine
HWL = length of right hind wing
HWW = maximum width of right hind wing
IE = width of synthlipsis, minimum distance measured between inner margins of compound eyes
LPSD = maximum distance of two lateral pronotal spines
LPSL = length of lateral pronotal spine
MFL = length of left mid femur
MTL = length of left mid tibia
NL = length of neck
OCD = minimum distance measured between inner margins of lateral ocelli
OD = maximum diameter of left ocellus
OE = maximum distance measured between outer margins of compound eyes
PFL = length of left hind femur
PnL = pronotal length
PnW = maximum pronotal width
PoL = length of postocular area of head
PoW = maximum width of postocular area of head
PPL = length of posterior pronotal lobe
PTL = length of left hind tibia
R+M = length of R + M of right hemelytron
R1L = length of first visible labial segment
R2L = length of second visible labial segment
R3L = length of third visible labial segment
Sc = length of Sc of right hemelytron

Morphometric analyses

Considering the weak to moderate sexual dimorphism of the external morphology of species of Reduviidae, the Principal Component Analyses (PCA) were performed separately for the female adult and male adult datasets using R software ver. 4.1.2 (R Core Team 2021). The two datasets were named as 'Female Morphometric dataset' and 'Male Morphometric dataset'. Both morphometric datasets comprised 39 morphological features (BL, HL, AoL, PoL, AoW, PoW, OE, IE, ED, OD, OCD,COD, R1L, R2L, R3L, HSL, HSD, neck length NL, A1L, A2L, A3L, A4L, PnL, PnW, APL, PPL, LPSD, LPSL, CPSL, HeL, HeW, Sc, R+M, AFL, ATL, MFL, MTL, PFL, and PTL).

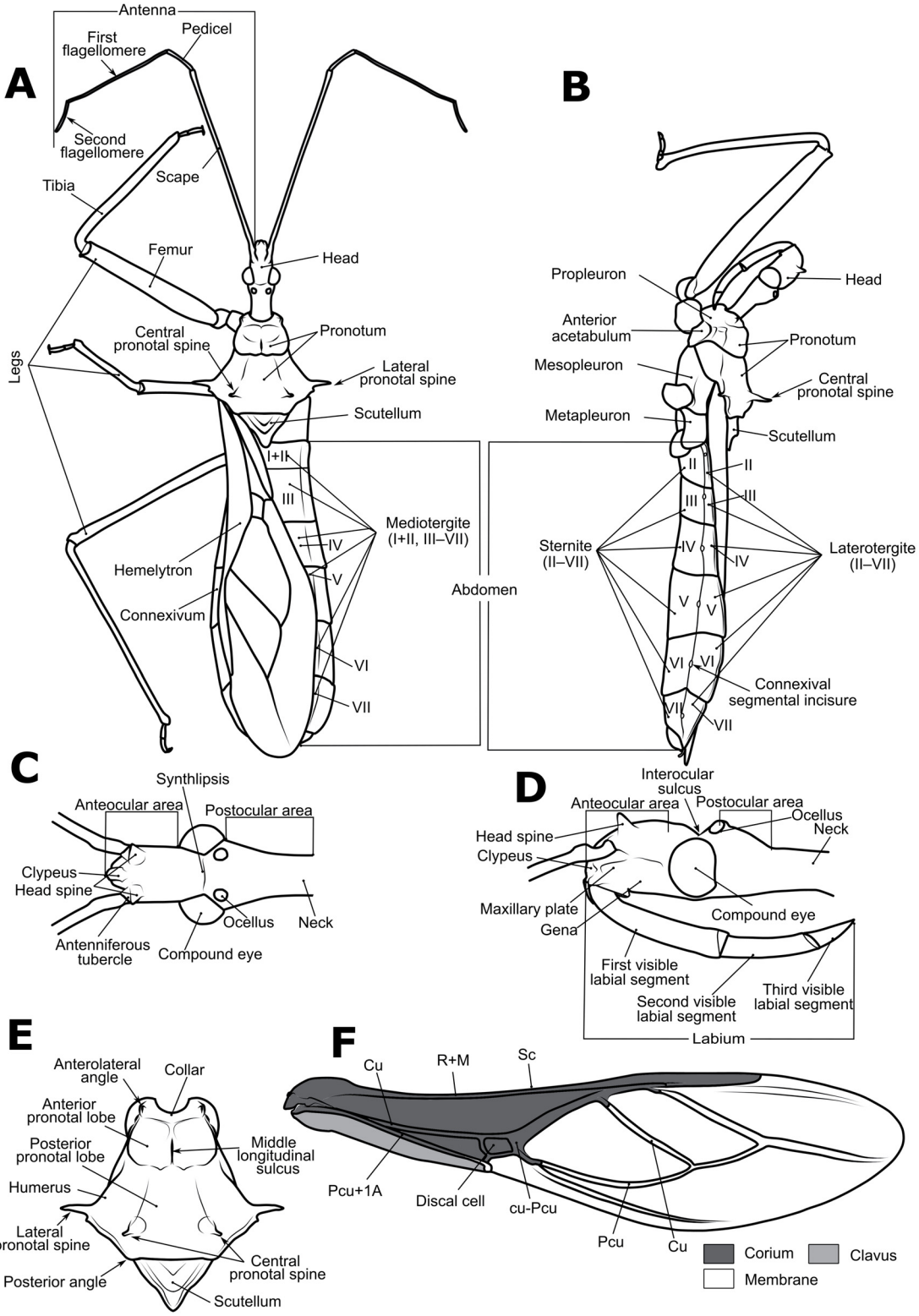

Fig. 1. Structure and morphological terms of species of *Epidaus* Stål, 1859. Drawing based on *Epidaus batxatensis* Truong, Nguyen & Ha sp. nov., holotype, ♂ (HNL2024-234). **A**. Body in dorsal view. **B**. Body in lateral view. **C**. Head in dorsal view. **D**. Head in lateral view. **E**. Pronotum and scutellum in dorsal view. **F**. Right hemelytron in dorsal view.

Moreover, due to our limited collection, there are only specimens of four species of *Epidaus* available for the morphometric analyses. Therefore, in order to enrich the morphometric dataset, we also attempted to employ the measurement data of *E. bachmaensis*, *E. insularis* Zhang, Zhao, Cao & Cai, 2010, and *E. wangi* Chen, Zhu, Wang & Cai, 2016 from their original description (obtained from the measurement sections or measured from their illustrations). Those measurement data were associated with our data and named as 'Extended Male Morphometric dataset'. This dataset comprises 30 morphometric features (BL, HL, AoL, PoL, AoW, PoW, OE, IE, ED, COD, R1L, R2L, R3L, HSL, HSD, A1L, A2L, A3L, A4L, PnL, PnW, APL, PPL, LPSD, LPSL, CPSL, HeL, HeW, Sc, R+M).

The function 'fviz_pca_ind' (factoextra package) (Kassambara & Mundt 2020) was used to graph the 2D plot of PCA.

Flowchart, raw morphometric datasets, and the R-scripts used for the data design and analyses are presented in additional files (Supp. files 1, 2, 3, 4, 5).

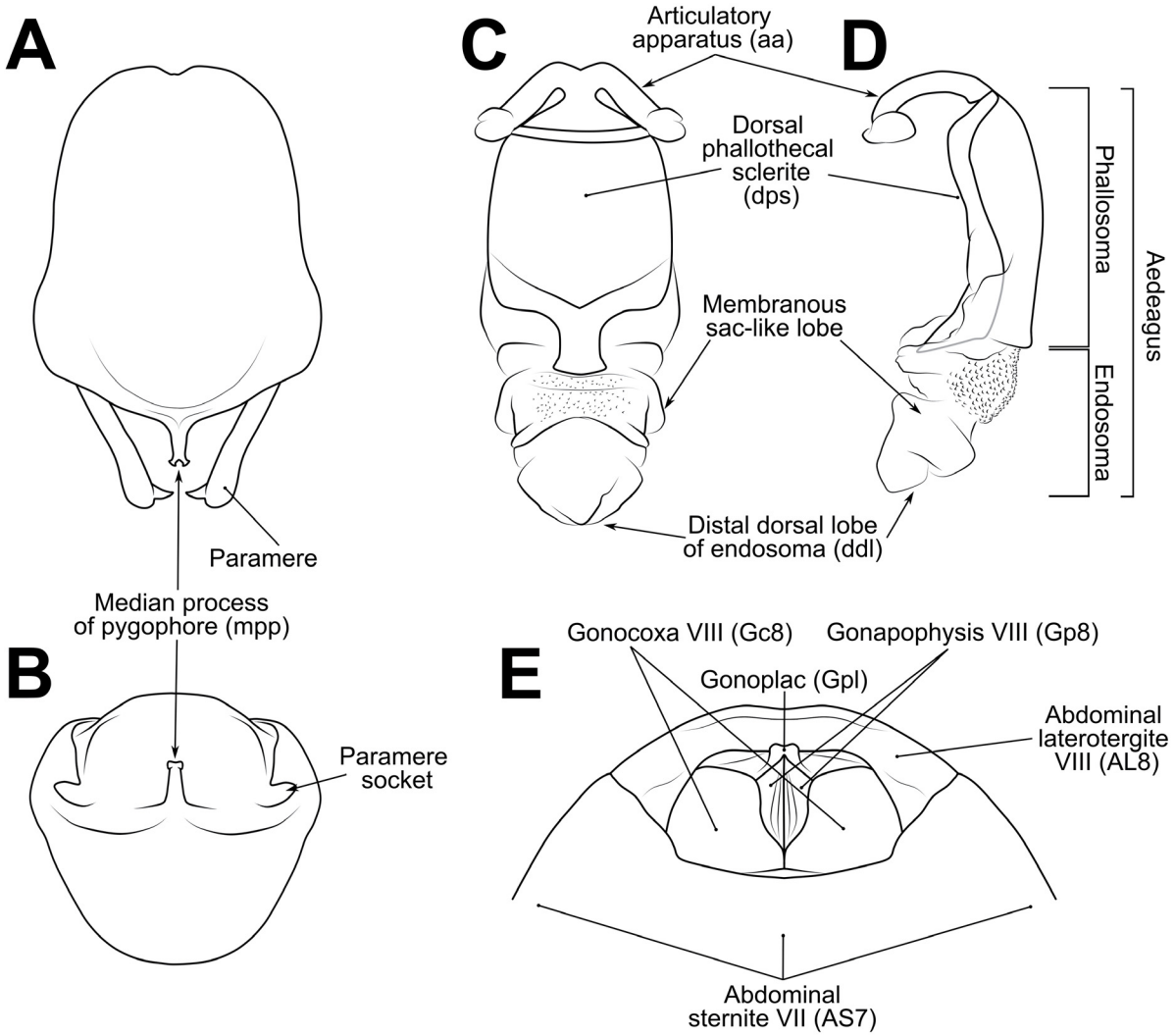

Fig. 2. Structure and morphological terms of species of *Epidaus* Stål, 1859 (cont.). Drawing based on *Epidaus batxatensis* Truong, Nguyen & Ha sp. nov. **A–D**. Holotype, ♂ (HNL2024-234). **E**. Paratype, ♀ (HNL2024-276). **A**. Pygophore with paramere of male genitalia in ventral view. **B**. Pygophore in caudal view. **C**. Phallus in dorsal view. **D**. Phallus in lateral view. **E**. Female external genitalia in ventral view.

Molecular data preparation

DNA was isolated from each specimen's right hind leg or right mid leg by the Chelex-TE-ProK protocol (Satria *et al.* 2015). The mitochondrial COI gene fragments were examined using the primer set of LCO1490m (5′-TAC TCA ACA AAT CAC AAA GAT ATT GG-3′) (Hajibabaei *et al.* 2006) and COI-E (5′-TAT ACT TCT GGG TGT CCG AAG AAT CA-3′) (Simon *et al.* 1994). Polymerase chain reaction (PCR) amplification, cycle sequencing reaction, sequencing using ABI PRISM 3130xl (Applied Biosystems), and sequence assembly using ChromasPro ver. 1.7.6 (Technelysium Pty Ltd., Australia) were executed using the methods of Simon *et al.* (1994), Hajibabaei *et al.* (2006) and Satria *et al.* (2015). The PCR thermal situation for the COI gene fragment, comprised of initial denaturation at 94°C (2 min),

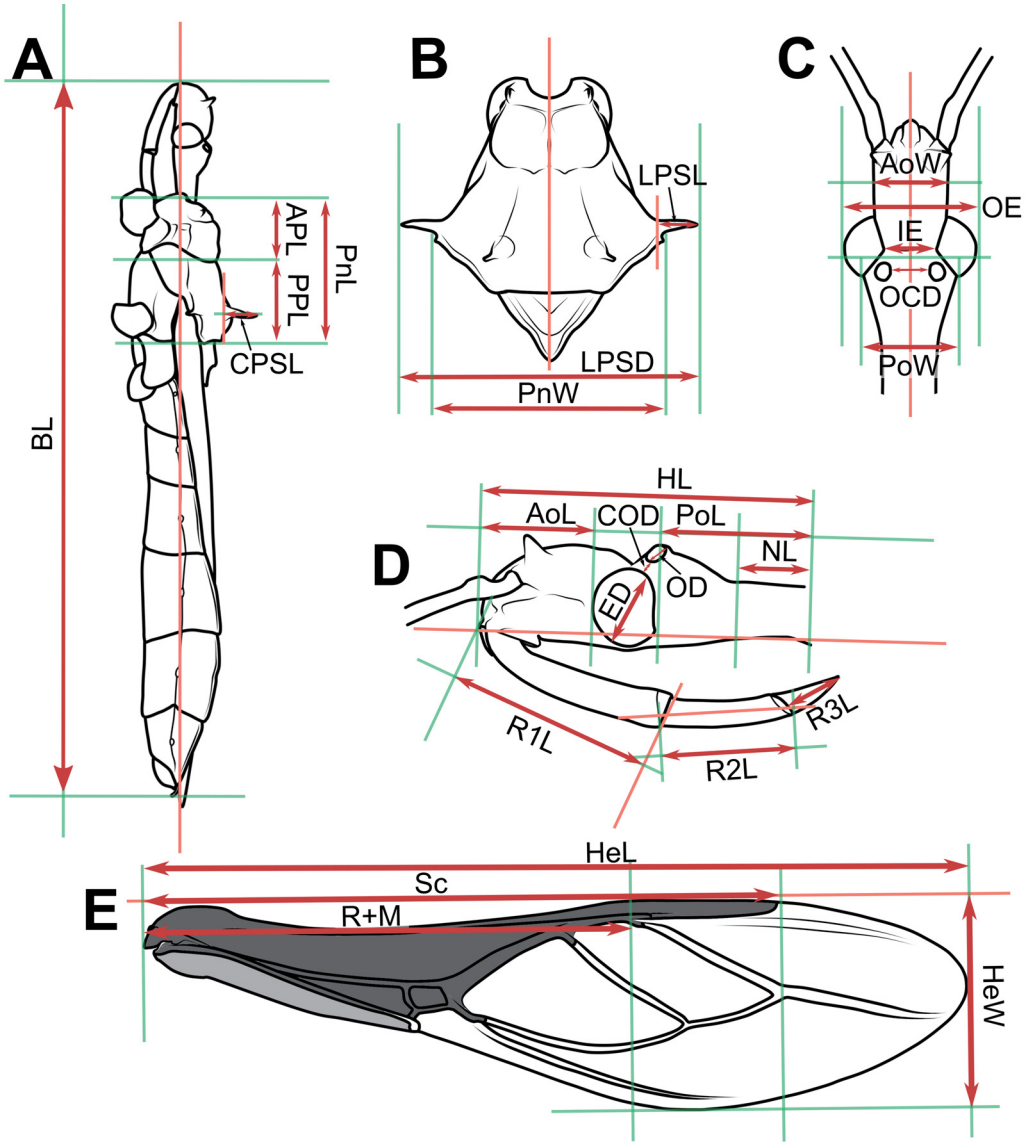

Fig. 3. Measurement characters of species of *Epidaus* Stål, 1859. Drawing based on *Epidaus batxatensis* Truong, Nguyen & Ha sp. nov., holotype, ♂ (HNL2024-234). **A**. Body in lateral view. **B**. Pronotum and scutellum in dorsal view. **C**. Head in dorsal view. **D**. Head in lateral view. **E**. Right hemelytron in dorsal view.

denaturation at 94°C (30 s), annealing at 48.5°C (30 s), and extension at 72°C (45 s) for 35 cycles, with final extension at 72°C (7 min). COI sequences were effectively obtained from all 32 samples of *Epidaus*.

Test for association was performed using MUSCLE implemented in MEGA X (Kumar *et al.* 2018) with default setting (Gap Open = -400.00; Gap Extend = 0.00; Cluster Method [Iterations 1,2 and Other iterations] = UPGMA; Min Diag Length [Lambda] = 24) for COI sequences while including and excluding outgroups (OG+ or OG−): $COI^{(OG+)}$ (624 bp) and $COI^{(OG-)}$ (624 bp) datasets. The FASTA-configured files derived from MEGA X were then converted to NEXUS layout or PHYLIP design, which were suitable input layouts for molecular phylogenetic examination and estimation of genetic distances and species delimitation analysis by ClustalX ver. 2.0.11 (Larkin *et al.* 2017).

Molecular phylogenetic analyses

Molecular phylogenetic analyses were done based on the COI dataset. The GTR + Gamma model was chosen for the COI dataset using Model Finder (Kalyaanamoorthy *et al.* 2017) under the Bayesian information criterion. The Bayesian Inference (BI) evaluations were then executed for the data using MrBayes ver. 3.2.7 (Ronquist & Huelsenbeck 2003) with 20 000 000 productions and statutory parameter configuration (examining every 500 generations and tuning constraints every 100 generations, with a burn-in of 25%). The ESS of each constraint was verified to be > 200 using Tracer ver. 1.7.2 (Rambaut *et al.* 2018). The nodes were designated as 'well supported' when the Posterior Probability of BI analysis (PP) ≥ 0.95.

Pairwise p-distances and Kimura-two-parameter (K2P) distances were calculated for the COI dataset of *Epidaus* using MEGA X (Kumar *et al.* 2018) under 'pairwise deletion'.

Species delimitation analyses

To create species partitions, two different protocols, i.e., Assemble Species by Automatic Partitioning (ASAP) (Puillandre *et al.* 2021) and Bayesian implementation of the Poisson Tree Processes model (bPTP) for species delimitation (Zhang *et al.* 2013), were used with pairwise genetic distances. For ASAP, the FASTA-configured file of the $COI^{(OG-)}$ dataset was used and executed on the ASAP website (https://bioinfo.mnhn.fr/abi/public/asap), with two replacement samples to estimate the distances, i.e., simple p-distance model and K2P model. The bPTP was executed in the bPTP online server (https://species.h-its.org) based on the NEXUS formatted BI tree of the $COI^{(OG-)}$ dataset, with default values (100 000 Markov chain Monte Carlo [MCMC] generations, thinning = 100, burn-in = 0.1, and Seed = 123). The NEXUS formatted BI tree used in bPTP was converted from TREE formatted by TreeGraph ver. 2.15.0-887 (Stöver & Müller 2010).

Results

Morphological examination

Out of the 41 specimens of *Epidaus* of the IB's heteropteran collection, two distinct morphospecies that could not be classified under any currently recognized *Epidaus* species based on their external morphological features and male genitalia characteristics were identified. The two morphospecies were then temporarily named morphospecies α and β (Fig. 4). The morphological differences between the newly described species and the previously known Vietnamese species of *Epidaus* were presented in Supp. file 6.

Morphometric analyses

Two species, *Epidaus bachmaensis* and *E. famulus*, and two morphospecies, α and β, were discriminated from each other by PCA based on the 'Male Morphometric dataset' (Fig. 5A). With the 'Extended Male Morphometric dataset', the two morphospecies, α and β, were discriminated well from each other and from other *Epidaus* species, *E. bachmaensis*, *E. famulus*, *E. insularis*, and *E. wangi* (Fig. 5B).

Similarly, PCA based on the 'Female Morphometric dataset', also revealed a significant separation of two morphospecies, α and β, and *E. bachmaensis* and *E. longispinus* (Fig. 6).

Unfortunately, mature specimens of *Epidaus sexspinus*, adult female specimens of *E. famulus*, and adult males of *E. longispinus* were unavailable for morphometric analyses.

Phylogenetic analyses and DNA barcoding

The phyologenetic analyses are based on the COI dataset comprising sequences of 34 Vietnamese specimens of *Epidaus* in this study associated with a COI sequence of *Epidaus tuberosus* Yang, 1940 obtained from GenBank (Table 1; Fig. 7). The Bayesian inference analyses (BI) recovered seven lineages (named lineages A–G) as independence or singleton lineages with high supporting values (PP ≥ 0.95) and long basal branch (lineages G) (Fig. 7). The minimum divergences between each pair of lineages ranged from 3.2% to 14.6% in p-distance and 0.033 to 0.163 in K2P (Table 2). Furthermore, the maximum diversity p-distance of each lineage ranged from 0.2% to 0.8% (0.002 to 0.008 in K2P) (Table 2).

The phylogenetic portioning of the seven lineages A–G was supported consistently by ASAP and bPTP based on the $COI^{(OG-)}$ dataset (Fig. 7).

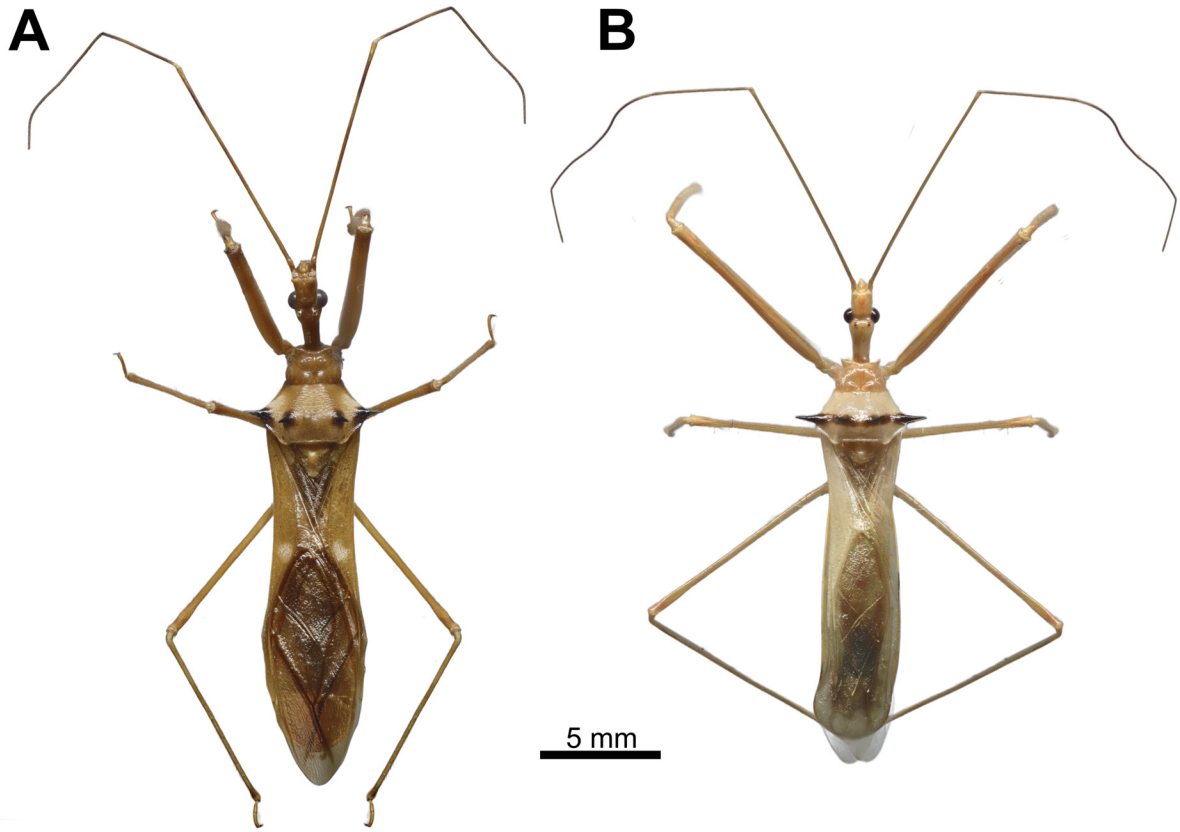

Fig. 4. Body in dorsal view of two new morphospecies, α and β. **A**. *Epidaus batxatensis* Truong, Nguyen & Ha sp. nov. (= α), paratype, ♂ (HNL2018-235). **B**. *E. konkakinhensis* Truong, Nguyen & Ha sp. nov. (= β), holotype, ♂ (TXL2022-148).

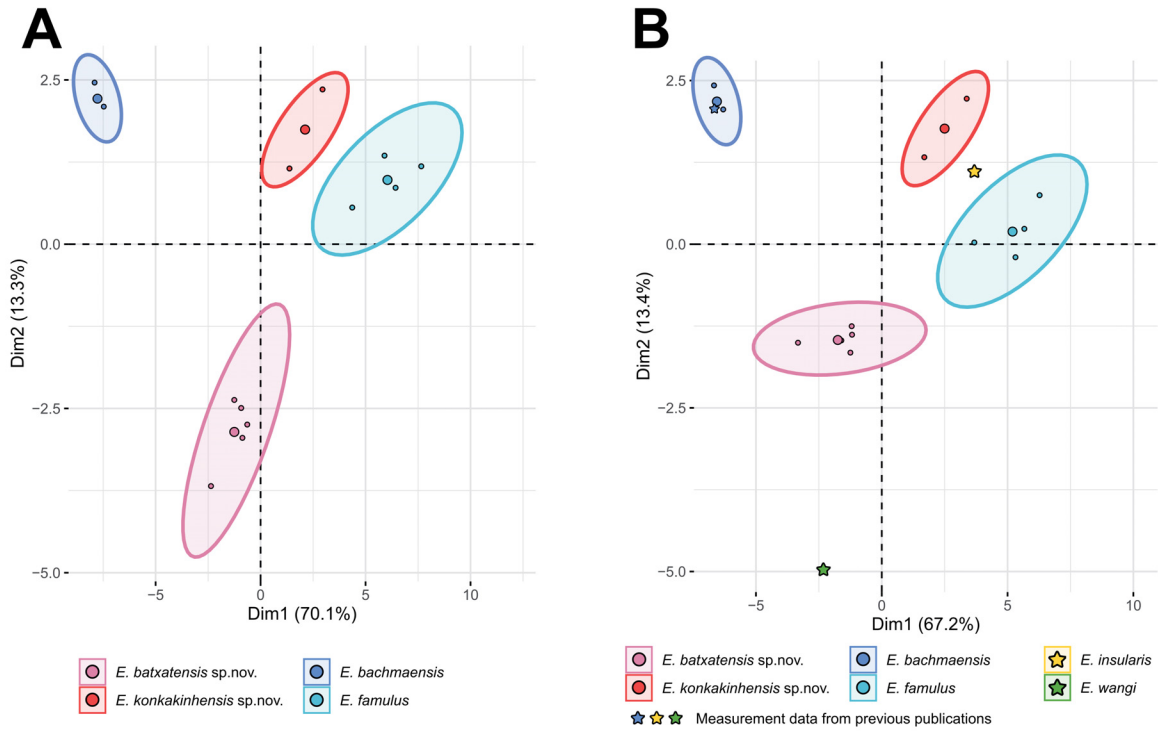

Fig. 5. 2D PCA-plots. **A**. Based on the 'Male Morphometric dataset'. **B**. Based from the 'Extended Male Morphometric dataset'.

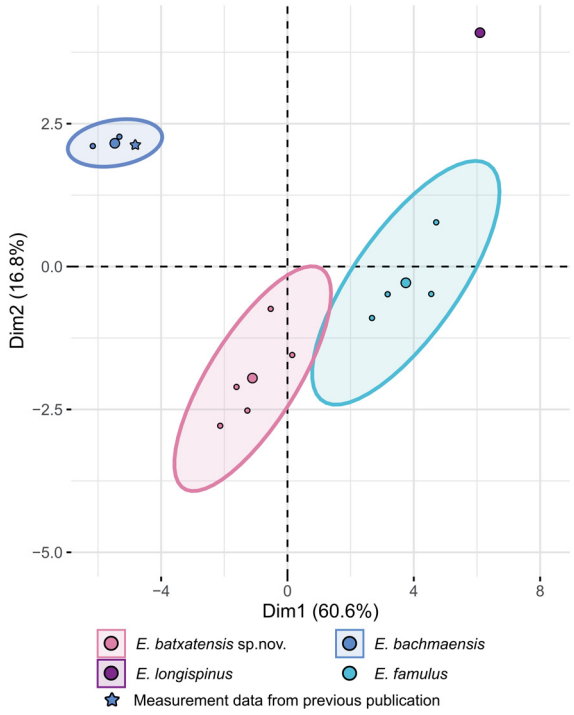

Fig. 6. 2D PCA-plots based on the 'Female Morphometric dataset'.

Species discrimination and identification

The independence of each morphospecies α and β was confirmed by morphometry, phylogenetic analysis, and species delimitation analyses. The two morphospecies α and β were also distinguished from 26 congeners of the genus *Epidaus*, including the following four species already recorded from Vietnam, i.e., *E. bachmaensis* (= lineage C), *E. famulus* (= lineage D), *E. longispinus* (= lineage E), and *E. sexspinus* (= lineage F), based on the characteristics of external and genital morphology. Therefore, the two morphospecies α and β were herein treated as two independent species, and then named and described as *Epidaus batxatensis* Truong, Nguyen & Ha sp. nov. and *Epidaus konkakinhensis* Truong, Nguyen & Ha sp. nov., respectively.

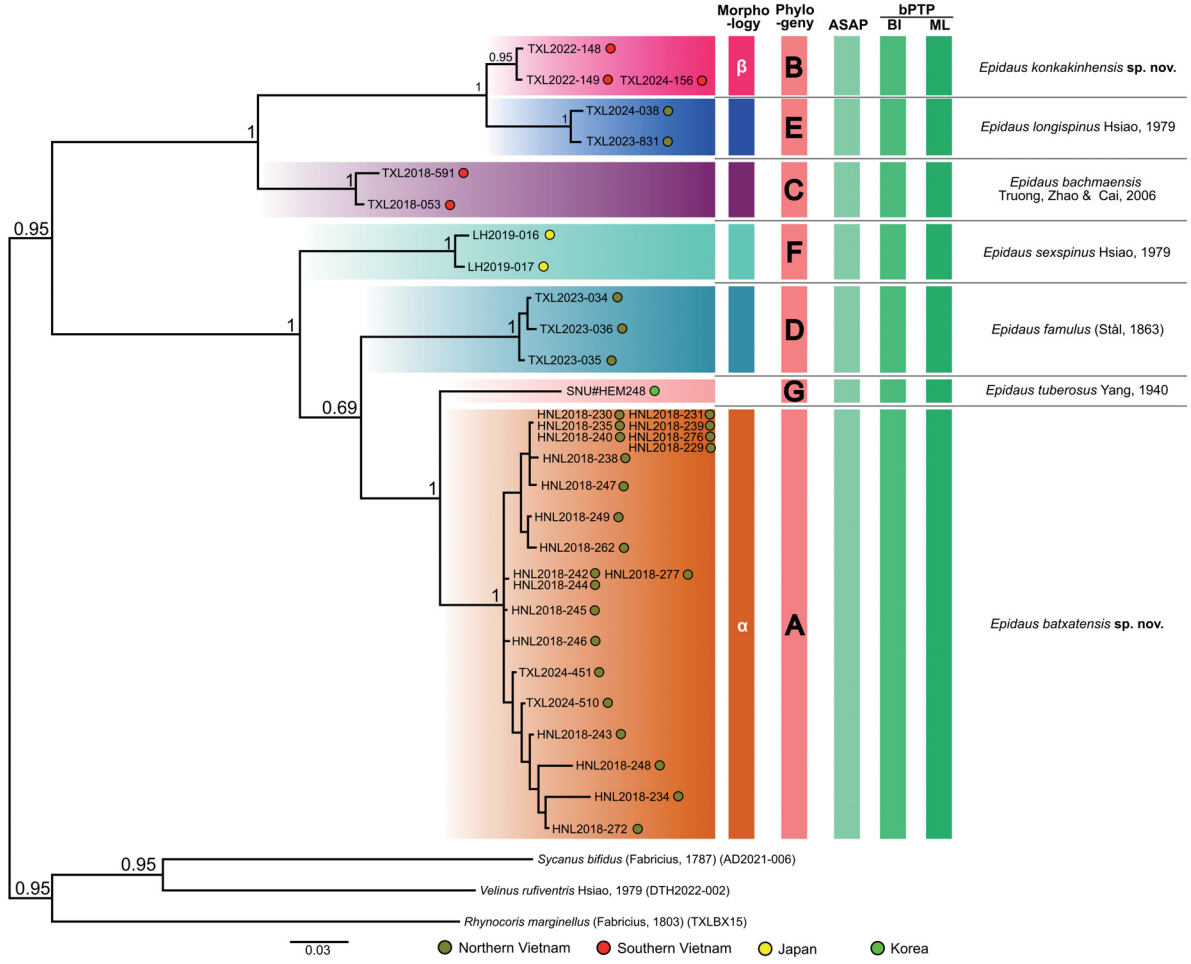

Fig. 7. Bayesian inference phylogenetic tree based on the COI dataset (546 bp) of species of *Epidaus* Stål, 1859 collected from Vietnam and the COI sequence of *Epidaus tuberosus* Yang, 1940 from GenBank. Posterior probability values are given beside the basal nodes. The tips are labeled with the voucher specimen IDs. The color circles on the right of each voucher specimen IDs illustrate the collection localities.

Table 2. Maximum intraspecific and minimum interspecific p-distance and K2P distances in analysed species of the genus *Epidaus* Stål, 1859 calculated based on the COI sequence dataset. The upper right diagonal shows the distance in the K2P model, and the lower left diagonal shows the p-distance (%). Abbreviations: max K2P = maximum distance in K2P model within the clade or singleton lineage; max p = maximum p distance within the clade or singleton lineage; N = number of specimens of the clade or singleton lineage.

	Species	A	B	C	D	E	F	G
A	*Epidaus batxatensis* sp. nov. (N = 20; max p = 0.2 %; max K2P = 0.002)		0.159	0.162	0.076	0.163	0.076	0.052
B	*Epidaus konkakinhensis* sp. nov. (N = 3; max p = 0.2 %; max K2P = 0.002)	14.3		0.093	0.145	0.033	0.145	0.155
C	*Epidaus bachmaensis* (N = 2; p = 0.8 %; K2P = 0.008)	14.6	8.7		0.147	0.106	0.151	0.156
D	*Epidaus famulus* (N = 3; max p = 0.3 %; max K2P = 0.003)	7.2	13.1	13.3		0.153	0.092	0.093
E	*Epidaus longispinus* (N = 2; p = 0.5 %; K2P = 0.005)	14.6	3.2	9.8	13.8		0.147	0.163
F	*Epidaus sexspinus* (N = 2; p = 0.5 %; K2P = 0.005)	7.2	13.1	13.6	8.7	13.3		0.095
G	*Epidaus tuberosus* (N = 1)	5.0	13.9	14.1	9.3	14.6	8.7	

Taxonomy

Class Insecta Linnaeus, 1758
Order Hemiptera Linnaeus, 1758
Suborder Heteroptera Latreille, 1810
Family Reduviidae Latreille, 1807
Subfamily Harpactorinae Amyot & Serville, 1843

Genus ***Epidaus*** Stål, 1859

Epidaus Stål, 1859: 193.
Gastroplaeus Costa, 1864: 140 (synonymized by Stål 1874).

Epidaus – Stål 1874: 9. — Distant 1904: 371. — Hsiao & Ren 1981: 498. — Putshkov & Putshkov 1985: 42; 1996: 239. — Maldonado-Capriles 1990: 198.

Type species

Zelus transversus Burmeister, 1835; by subsequent designation (Distant 1904: 371).

Distribution

Oriental and Sino-Japanese regions.

Epidaus batxatensis Truong, Nguyen & Ha sp. nov.
urn:lsid:zoobank.org:act:A8940EEC-D697-4AB3-969A-34F8225B7ECA
Figs 1, 2A–D, 3, 4A, 5–10

Diagnosis

Body yellowish brown to brown; scape brown with two yellowish brown suffusions in basal 2/5 and basal 4/5, pedicel brown with basal 1/5 and basal 4/5 regions yellowish brown, and apical region dark brown, first and second flagellomeres blackish brown; head spine behind antenniferous tubercle small (0.40–0.50 mm) and far from each other (0.96–1.12 mm); posterior pronotal lobe rugulose and punctured, yellowish brown, except anterolateral margin and two weak longitudinal elevations dark brown; four pronotal spines black, large and well produced (0.80–1.20 mm); coria yellow or yellowish brown with a large white spot in posterior apex when being fresh; laterotergites yellowish brown with posterior 1/4 of laterotergite V and anterior margin of laterotergite VI suffused with dark brown.

Differential diagnosis

This species is very similar to *Epidaus famulus* in general appearance, especially in body color and the presence of white spots when fresh. But the new species can be distinguished from *E. famulus* by a combination of the following characteristics: laterotergites yellowish brown with posterior 1/4 of laterotergite V and anterior margin of laterotergite VI suffused with dark brown (Fig. 8B) (in *E. famulus* laterotergites brown or yellowish brown with posterior 1/2 of laterotergite V and anterior 1/4 of laterotergite VI blackish brown), lateral area of pronotum and posterior apex of coria with very large white spot, scutellum without any white spot (in *E. famulus* lateral and posterior area of pronotum, disk of scutellum, corium with small round white spots), femora with apical 1/3 suffused with two brown or dark brown bands (in *E. famulus* femora entirely brown), posterior margin of dorsal phallothecal sclerite strongly spoon-liked produced in dorsal view (Fig. 10D) (in *E. famulus* that posterior margin is slightly prominent, not posteriorly produced).

Etymology

The specific epithet refers to its occurrence in Bat Xat Natural Reserve, an adjective.

Type material

Holotype

VIETNAM – **Lao Cai Province** • ♂; Bat Xat Natural Reserve; 26 Jul. 2024; N.L. Ha leg.; IB-DEB, HNL2024-234.

Paratypes

VIETNAM – **Lao Cai Province** • 8 ♂♂; same data as for holotype; IB-DEB, HNL2024-230, HNL2024-231, HNL2024-235, HNL2024-239, HNL2024-240, HNL2024-242, HNL2024-244, HNL2024-245 • 5 ♀♀; same data as for holotype; IB-DEB, HNL2024-238, HNL2024-243, HNL2024-272, HNL2024-276, HNL2024-277.

Non-type material

VIETNAM – **Lai Chau Province** • 1 ♀; Tam Duong, Ta Leng; 28 Mar. 2024; X.L. Truong leg.; IB-DEB, TXL2024-451 • 1 ♀; Tam Duong, Then Sin; 1 Apr. 2024; X.L. Truong leg.; IB-DEB, TXL2024-510. – **Lao Cai Province** • 3 ♂♂; same data as for holotype; IB-DEB, HNL2024-247, HNL2024-249, HNL2024-262 • 3 ♀♀; same data as for holotype; IB-DEB, HNL2024-229, HNL2024-246, HNL2024-248.

Type locality

Vietnam, Lao Cai Province, Bat Xat Natural Reserve.

Description

Male

Coloration. Body yellowish brown to brown. Head yellowish brown, except dorsal anterocular area of head, base of neck, gena, and head venter brown; two longitudinal stripes in centre of anteocular area of head; first visible labial segment yellowish brown; second visible labial segment luteous; basal half of third visible labial segment luteous or pale yellowish brown, remaining brown (Fig. 8C–D). Scape brown with two yellowish brown suffusions in basal 2/5 and basal 4/5; pedicel brown with basal 1/5 and basal 4/5 regions yellowish brown, and apical region dark brown; first and second flagellomeres blackish brown. Collar, anterolateral angle, anterior pronotal lobe, anterior acetabulum, meso- and metapleural, and sterna brown; anterior pronotal lobe with patterned dark yellowish brown suffusions (Fig. 9A); stridulatory sulcus luteous; posterior pronotal lobe yellowish brown, except anterolateral margin dark brown (Fig. 9A); lateral pronotal spines and central pronotal spines blackish brown or black (Fig. 9A); scutellum yellowish brown with centrally suffused with brown (Fig. 9A); propleuron yellowish brown; coxae brown; trochanters yellowish brown; femora, tibiae, and tarsi yellowish brown; femora with apical 1/3 suffused with two brown or dark brown bands. Coria yellow or yellowish brown; clavus yellowish brown except posterior 1/3 semi-transparent (Fig. 9B); membrane pale bronzy brown, semi-hyaline (Fig. 9B). Hind wings faintly semi-hyaline (Fig. 9C). Abdominal mediotergites and laterotergites yellowish brown; posterior 1/4 of laterotergite V and anterior margin of laterotergite VI suffused with dark brown (Fig. 8B); abdominal sternites brown. Pygophore brownish yellow. Lateral and posterior areas of pronotum and posterior apex of coria largely spotted with cretaceous-white, but those spots often fainted or disappeared after being preserved in ethanol.

Structure. Body large-sized (21.39–24.04 mm), elongated and posteriorly slightly widened (Fig. 8A–B). Head tubular, slender, elongated (Fig. 8C–D); anteocular area of head elongate-conical; anteclypeus sub-cylindrical and slightly prominent; postocular area of head globose, distinctly wider than anteocular area, shorter than anteocular area, constricted behind compound eyes, with a wide and deep interocular sulcus; neck short (0.80–0.93 mm) (Fig. 8C–D). Compound eyes protruding laterally, nearly globose, with posterior margin sub-straight, oblique with respect to ventral margin of head; lateral ocelli produced, slightly elevated behind interocular sulcus, separated from each other; interspace between lateral ocelli wider than distance between compound eye and lateral ocellus (Fig. 8C–D). First visible labial segment slightly thicker and longer than second segment, longer than anteocular area of head, extending beyond posterior margin of compound eye when labium laid backward (Fig. 8D); proportional average length of first to third visible labial segments 2.3 : 1.5 : 0.7. Scape very long, about 2.6 times as long as head, about 2.0 times as long as pedicel, slightly longer than first and second flagellomeres together; first flagellomere slightly longer than pedicel, and nearly 3 times as long as second flagellomere; proportional average length of scape, pedicel, first and second flagellomeres 9.9 : 5.1 : 6.9 : 2.6. Collar thick in dorsal view, submerged medially, with anterolateral angle roundly produced anteriorly; anterior pronotal lobe small, hemisphered and bulged, smooth, deeply depressed at base; posterior pronotal lobe rugulose and punctured, shallowly depressed on disc with two large central pronotal spines; two weak longitudinal elevations from anterior margin of posterior pronotal lobe to central pronotal spine of each side; humerus triangular, with a large laterally produced spine in lateral apex of each side; two central pronotal spines and two humerus spines formed a transverse row in basal 2/3 of posterior pronotal lobe; posterior margin of pronotum weakly convex; posterior angles round, slightly exceeding posterior margin of pronotum (Fig. 9A). Scutellum triangular, triangularly depressed basally, and sloping downward, posterior apex round and slightly posteriorly produced (Fig. 9A). Femora elongated, slender but stout, moderate subnodulose apically, apical margin of femora with small spines evenly; tibiae slender and elongated.

Hemelytra surpassing beyond apex of abdomen when fully closed, 0.7 times as long as body length (Fig. 9A); discal cell nearly diamond-shaped, longer than wide (Fig. 9B); Sc 0.8 times as long as hemelytron length, 1.3 times as long as R+M (Fig. 9B). Hind wing about 3.4 times as long as maximum width (Fig. 9C). Laterotergites slightly dilated and ascending with segmental incisures, postero-lateral

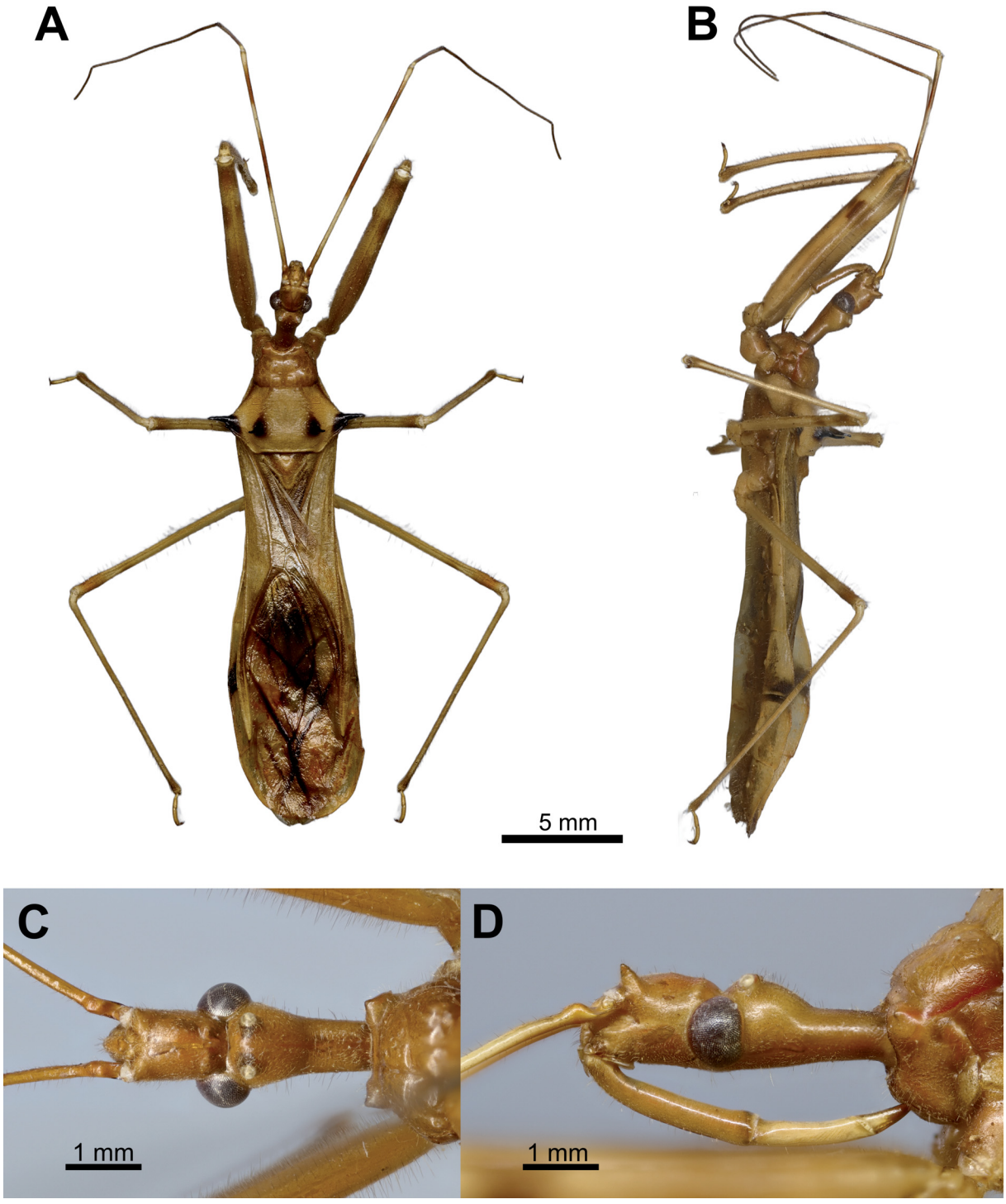

Fig. 8. *Epidaus batxatensis* Truong, Nguyen & Ha sp. nov., holotype, ♂ (HNL2024-234). **A**. Body in dorsal view. **B**. Body in lateral view. **C**. Head in dorsal view. **D**. Head in lateral view.

margin of each laterotergite not exceeding antero-lateral margin of following laterotergite (Fig. 8A–B). Pygophore ovoid (Fig. 10A–C); median process of pygophore (mpp) posteriorly produced, 0.46 times as long as wide in ventral view, with apical margin bifid, apicolateral corner specifically formed posterolaterad and blunt at apex (Fig. 10A–C); paramere long, slender, clavate, somewhat incurved in apical part, with round apex and inward-facing thorn (Fig. 10A). Aedeagus in dorsal view ovoid, dorsally sclerotized, and in lateral view long and narrow (Fig. 10D–F); articulatory apparatus in ventral view with basal plate arms relatively slender and jointly forming a V-shape, and in lateral view arched strongly (Fig. 10D–F); dorsal phallothecal sclerite in lateral view with posteromedian weakly produced and posterior margin strongly spoon-liked produced in dorsal view (Fig. 10F); spoon-like sclerites dissipated (Fig. 10D–F); membranous sac-like lobes almost disappeared (Fig. 10D–F); distal dorsal lobe of endosoma round and weakly bulged, with two large bulges densely covered with tiny and small prickles (Fig. 10G).

Vestiture. Body clothed with yellow setae. Head densely covered with short, slender, bent setae, interleaved with short, slender, erect setae; labium covered with short, slender, erect setae (Fig. 8C–D). Scape and pedicel covered with short, slender, sub-erect setae; remaining antennae covered with short, vertical setae, denser toward tip. Collar, anterolateral angles with tiny setae; anterior pronotal lobe with some rows of tiny bent setae, somewhat interleave with slender, erect setae; posterior pronotal lobe covered with short, slender, bent setae and somewhat interleaved with slender, erect setae; scutellum densely covered with short, slender, bent setae and interleaved with long slender erect setae (Fig. 6A). Coxae and trochanters covered with short, bent setae; femora, tibiae, and tarsi densely covered with long, slender, erect setae. Coria and clavus densely covered with short, bent setae. Abdominal mediotergites, laterotergites, and sternites sparsely covered with slender erect setae. Male genitalia pygophore ventrally basally and laterally covered with short, slender, bent setae and posteriorly densely covered with short and long, slender setae (Fig. 10A–C); base of paramere almost glabrous, remaining part of paramere densely covered with short and long, thick, erect setae (Fig. 10A).

Female

General external morphology similar to that of the male.

Coloration. Almost similar to males but differ in the following characters. Abdominal sternite VII brown with laterotergite VII yellowish brown; gonocoxa VIII (Gc8), gonapophysis VIII (Gp8), gonaplac (Gpl),

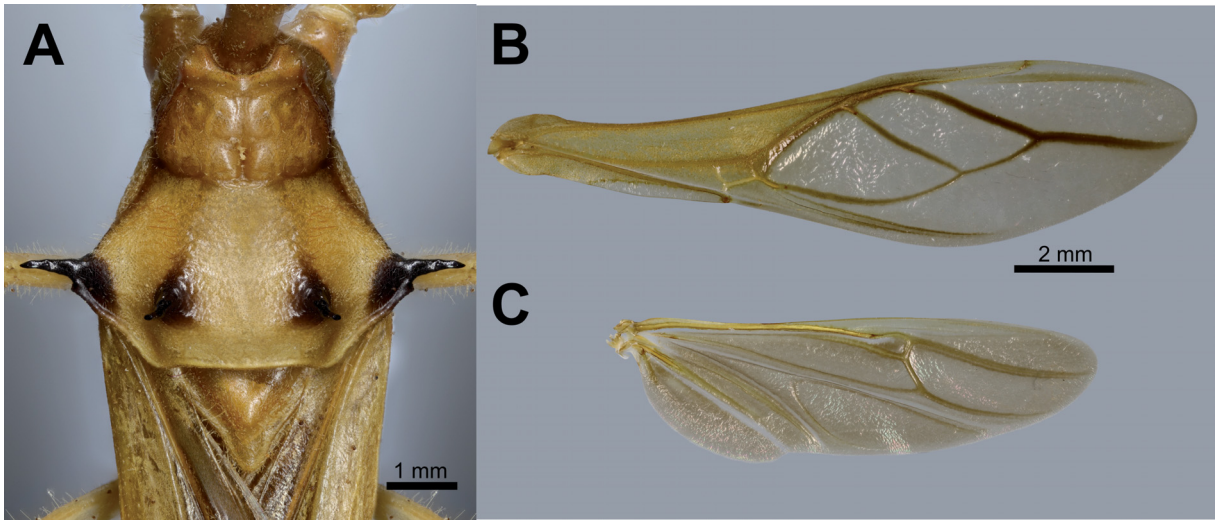

Fig. 9. *Epidaus batxatensis* Truong, Nguyen & Ha sp. nov., holotype, ♂ (HNL2024-234). **A**. Pronotum and scutellum in dorsal view. **B**. Right hemelytra. **C**. Right hind wing.

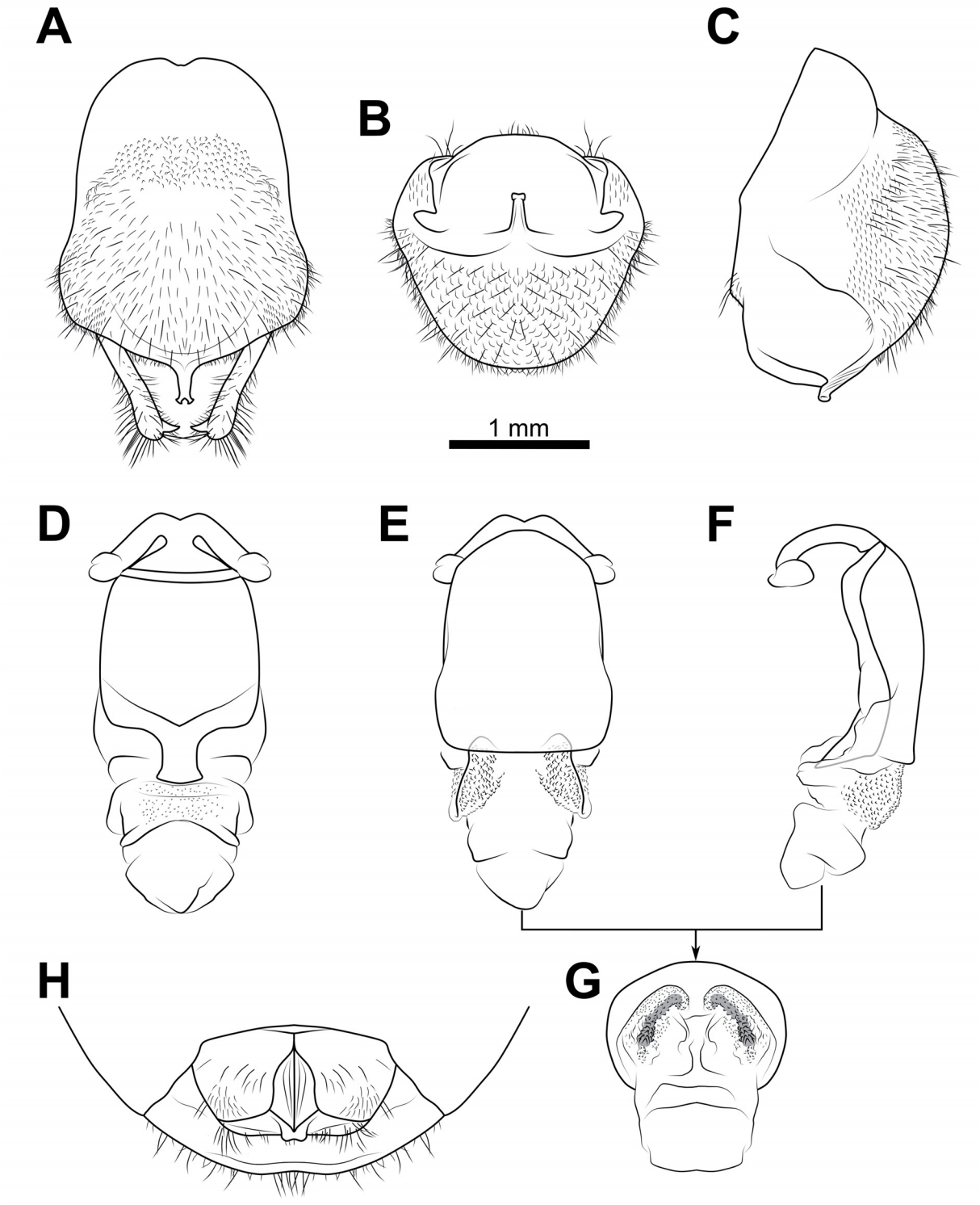

Fig. 10. *Epidaus batxatensis* Truong, Nguyen & Ha sp. nov. **A–G**. Holotype, ♂ (HNL2024-234), genitalia. **H**. Paratype, ♀ (HNL2024-276). **A–C**. Pygophore. **A**. Pygophore with paramere in ventral view. **B**. Pygophore in caudal view. **C**. Pygophore in lateral view. **D–F**. Aedeagus with endosoma semi-everted dorsal view. **D**. Dorsal view. **E**. Ventral view. **F**. Lateral view. **G**. Distal dorsal lobe of endosoma. **H**. Genitalia in ventral view.

and abdominal tergite IX (AT9) brown with irregular yellowish brown suffusions; abdominal laterotergite VIII (AL8) yellowish brown.

Structure. Almost the same as males but larger than males and differ in the following characters. Body large-sized (23.32–24.92 mm), elongated, and somewhat robust. Proportional average length of first to third visible labial segments 2.6 : 1.7 : 0.7. Scape about 2.5 times as long as head, about 2.0 times as long as pedicel, almost as long as first and second flagellomeres together; proportional average length of scape, pedicel, first and second flagellomeres 10.1 : 5.1 : 7.0 : 3.2. Abdominal laterotergite VIII (AL8) thick, with weakly reflexed posterior margin; abdominal sternite VII (AS7) forming a semi-circular or wide sub-pentagonal median concavity, with posteromedian margin gently U-shaped, with inner posterolateral margin slightly concave; gonocoxa VIII (Gc8) sub-rectangle, produced apical inner corner blunt, and with inner margin weakly incurved in posterior $^2/_3$; gonapophysis VIII (Gp8) subtriangular, posteriorly produced; abdominal tergite IX (AT9) not bulged and spoon-liked produced in middle of anterior margin (Fig. 10H).

Vestiture. Almost the same as males except for the following characteristics. Gonocoxa VIII (Gc8) sparsely covered with short and long, thick, erect setae; posterior margin of gonapophysis VIII (Gp8) somewhat covered with short, erect setae; abdominal tergite IX (AT9) densely covered with short and long, thick, erect setae; abdominal laterotergite VIII (AL8) marginally covered with short, bent, sub-erect setae and long, thick, erect setae (Fig. 10H).

Measurements (all dimensions are given in mm)

Holotype (♂)

BL 21.75; HL 4.04; AoL 1.44; AoW 0.90; PoL 0.90; PoW 1.14; NL 0.93; OE 1.67; IE 0.73; ED 0.84; OD 0.26; OCD 0.50; COD 0.20; R1L 2.50; R2L 1.70; R3L 0.74; A1L 9.72; A2L 5.13; A3L 6.70; A4L 2.39; HSL 0.50; HSD 0.96; PnL 4.37; PnW 4.79; LPSD 6.38; APL 1.65; PPL 2.69; LPSL 0.97; CPSL 1.21; HeL 14.24; HeW 3.63; Sc 10.95; R+M 8.40; HWL 9.65; HWW 2.88; AFL 8.37; ATL 8.14; MFL 6.92; MTL 7.88; PFL 9.49; PTL 10.70.

Paratypes (♂♂)

BL 21.39–21.80; HL 3.52–3.78; AoL 1.29–1.32; AoW 0.91–0.95; PoL 0.68–0.85; PoW 1.13–1.17; NL 0.80–0.89; OE 1.65–1.69; IE 0.72–0.80; ED 0.83–0.86; OD 0.24–0.31; OCD 0.52–0.57; COD 0.16–0.21; R1L 2.19–2.34; R2L 1.47–1.57; R3L 0.65–0.69; A1L 9.81–10.08; A2L 4.97–5.15; A3L 6.54–7.15; A4L 2.39–2.75; HSL 0.37–0.46; HSD 0.98–1.00; PnL 3.81–4.11; PnW 4.32–4.47; LPSD 5.65–5.82; APL 1.28–1.58; PPL 2.45–2.54; LPSL 0.92–1.01; CPSL 0.82–1.01; HeL 14.37–15.28; HeW 3.69–4.02; Sc 11.36–11.78; R+M 8.47–8.98; AFL 8.64–8.98; ATL 7.92–8.58; MFL 6.68–7.79; MTL 7.51–7.88; PFL 9.67–10.07; PTL 11.00–11.59.

Paratypes (♀♀)

BL 23.32–24.92; HL 3.90–4.13; AoL 1.40–1.49; AoW 1.00–1.06; PoL 0.83–0.99; PoW 1.24–1.27; NL 0.87–0.95; OE 1.71–1.80; IE 0.82–0.88; ED 0.86–0.93; OD 0.21–0.22; OCD 0.54–0.64; COD 0.20–0.25; R1L 2.48–2.67; R2L 1.65–1.79; R3L 0.65–0.79; A1L 9.64–10.37; A2L 4.73–5.37; A3L 6.38–7.36; A4L 3.17–4.82; HSL 0.32–0.43; HSD 1.04–1.12; PnL 4.30–4.91; PnW 4.80–5.10; LPSD 5.65–5.82; APL 1.57–1.91; PPL 2.69–3.04; LPSL 0.94–1.02; CPSL 0.89–1.12; HeL 15.93–17.67; HeW 4.22–4.65; Sc 12.57–13.50; R+M 8.64–9.85; AFL 9.04–10.85; ATL 8.43–9.78; MFL 7.21–7.73; MTL 7.88–8.49; PFL 9.53–11.13; PTL 11.62–12.63.

Distribution

Vietnam, Northern Regions (Lao Cai & Lai Chau provinces).

Epidaus konkakinhensis Truong, Nguyen & Ha **s**p. nov.
urn:lsid:zoobank.org:act:A32FDE86-2354-4730-872A-B99298A0FA32
Figs 4B, 11–13

Diagnosis

Body large-sized, pale luteous; scape very long, about 3.3 times as long as head, about 2.3 times as long as pedicel, about as long as first and second flagellomeres together, first flagellomere nearly 2.7 times as long as second flagellomere, scape and pedicel pale orangish yellow, first and second flagellomeres dark brown; collar thick in dorsal view, submerged medially, with anterolateral angle thorn-shaped produced anteriorly; posterior pronotal lobe punctured with posterior margin weakly concave, medially submerged; lateral pronotal spines and central pronotal spines blackish brown and surrounded by dark brown suffusions; scutellum pale brown, roundly triangular, triangularly depressed basally, and sloping downward, posterior apex round; abdominal sternites luteous, somewhat with irregular brown or orange suffusions

Differential diagnosis

This species is highly similar to *Epidaus longispinus* in general appearance, especially in body color and structures, and also has a very close relationship in molecular phylogeny (3.2% based on COI barcode). But the new species can be distinguished from *E. longispinus* by a combination of the following characteristics: body large size (19.2–20.5 mm in male) (in *E. longispinus* body large size but slightly smaller (20.3 mm in female)); posterior pronotal lobe without any longitudinal ridges (in *E. longispinus* posterior pronotal lobe with two short longitudinal ridges on the front edge); abdominal sternites luteous, somewhat with irregular brown or orange suffusions (Fig. 11B) (in *E. longispinus* abdominal sternites with brown broad longitudinal band on each side).

Etymology

The specific epithet refers to its occurrence in Kon Ka Kinh National Park, an adjective.

Type material

Holotype

VIETNAM – **Gia Lai Province** • ♂; Kon Ka Kinh National Park; 26 Mar. 2022; X.L. Truong leg.; IB-DEB, TXL2022-148.

Paratype

VIETNAM – **Gia Lai Province** • 1 ♂; same data as for holotype; IB-DEB, TXL2022-149.

Non-type material

VIETNAM – **Gia Lai Province** • 1 ♂; same data as for holotype; IB-DEB, TXLBXN4. – **Thua Thien Hue Province** • 1 ♂; Bach Ma National Park; 3 Feb. 2024; X.L. Truong leg.; IB-DEB, TXL2024-156.

Type locality

Vietnam, Gia Lai Province, Kon Ka Kinh National Park.

Description

Male

Coloration. Body pale luteous. Head pale orangish yellow, except dorsal anterocular area of head and base of neck yellowish brown; dorsal anteocular area of head with medially longitudinal orange strip; gena pale orangish yellow with a central orangish suffusion; first and second visible labial segments pale yellow; third labial segment brown with yellowish brown basally (Fig. 11C–D). Scape and pedicel pale orangish yellow; first and second flagellomeres dark brown. Collar, anterolateral angle, propleuron,

coxae, and anterior pronotal lobe pale orangish yellow; anterior pronotal lobe with irregular orange suffusions (Fig. 12A); posterior pronotal lobe pale luteous (Fig. 12A); lateral pronotal spines and central pronotal spines blackish brown and surrounded by dark brown suffusions (Fig. 12A); scutellum pale brown with pale luteous margins (Fig. 12A); anterior acetabulum, meso- and metapleural, and sterna pale brownish yellow; stridulatory sulcus pale luteous; trochanters yellowish brown; anterior femora yellowish brown with some longitudinal brown stripes; mid- and posterior femora, tibiae, and tarsi pale luteous. Coria pale luteous; clavus yellowish brown except posterior $^{2}/_{3}$ semi-transparent (Fig. 12B);

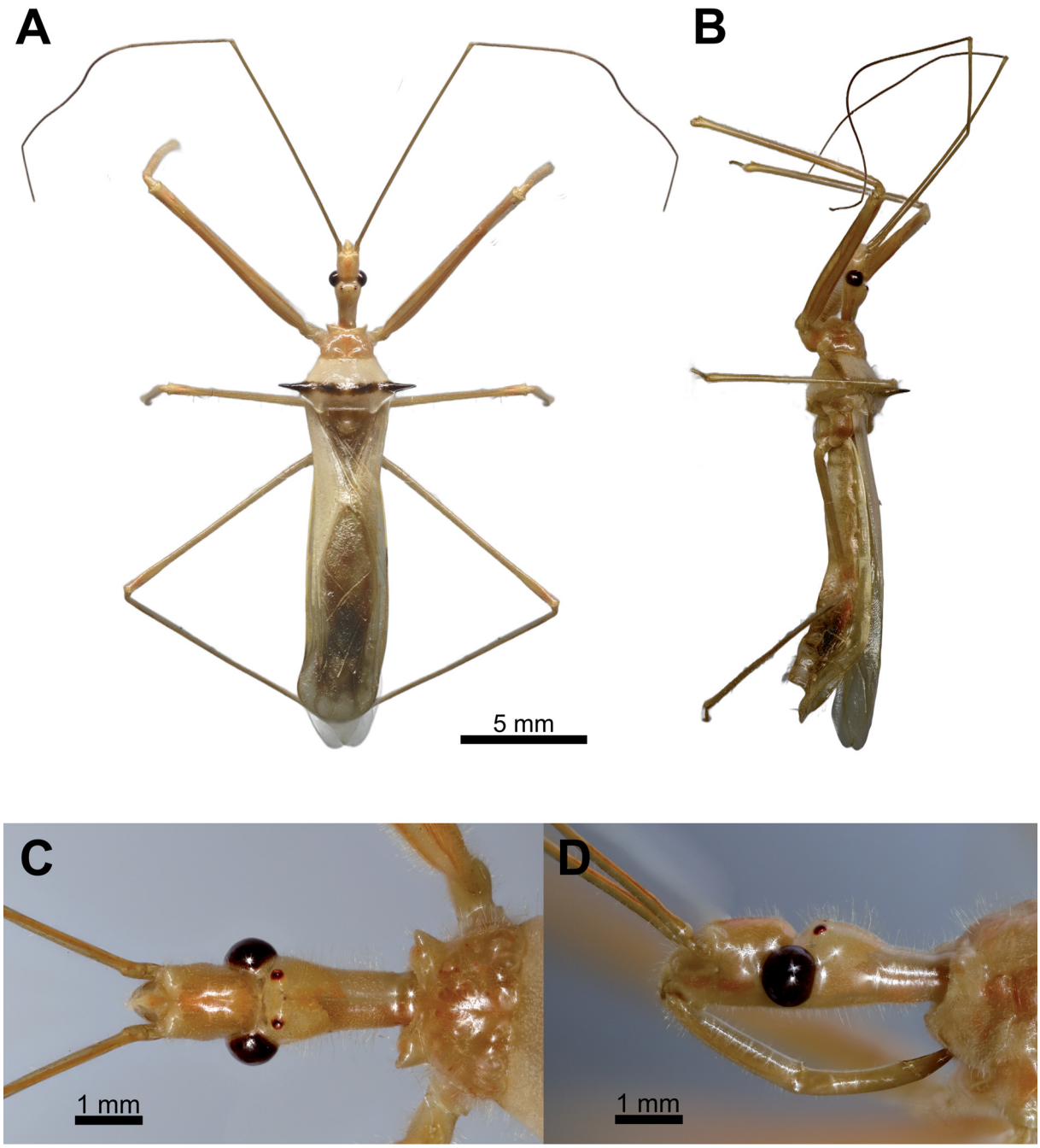

Fig. 11. *Epidaus konkakinhensis* Truong, Nguyen & Ha sp. nov., holotype, ♂ (TXL2022-148). **A**. Body in dorsal view. **B**. Body in lateral view. **C**. Head in dorsal view. **D**. Head in lateral view.

membrane pale bronzy brown, semi-hyaline (Fig. 12B). Hind wings faintly semi-hyaline (Fig. 12C). Abdominal mediotergites and laterotergites pale luteous (Fig. 11B); abdominal sternites luteous, somewhat with irregular brown or orange suffusions. Pygophore luteous.

Structure. Body large-sized (19.16–20.49 mm), elongated and posteriorly slightly widened (Fig. 11A–B). Head tubular, slender, elongated (Fig. 11C–D); anteocular area of head elongate-conical; anteclypeus sub-cylindrical and slightly prominent; postocular area of head globose, distinctly wider than anteocular area, slightly shorter than anteocular area, constricted behind compound eyes, with a wide and deep interocular sulcus; neck short (0.59–0.77 mm) (Fig. 11C–D). Compound eyes protruding laterally, nearly globose, with posterior margin sub-straight, oblique with respect to ventral margin of head; lateral ocelli weakly produced, slightly elevated behind interocular sulcus, separated from each other; interspace between lateral ocelli wider than distance between compound eye and lateral ocellus (Fig. 11C–D). First visible labial segment slightly thicker and longer than second segment, longer than anteocular area of head, nearly extending beyond posterior margin of compound eye when labium laid backward (Fig. 11D); proportional average length of first to third visible labial segments 1.9 : 1.5 : 0.6. Scape very long, about 3.3 times as long as head, about 2.3 times as long as pedicel, about as long as first and second flagellomeres together; first flagellomere nearly 2.7 times as long as second flagellomere; proportional average length of scape, pedicel, first and second flagellomeres 10.7 : 4.6 : 7.8 : 2.9. Collar thick in dorsal view, submerged medially, with anterolateral angle thorn-shaped produced anteriorly; anterior pronotal lobe small, hemisphered and bulged, smooth, deeply depressed at base; posterior pronotal lobe punctured, shallowly depressed on disc with two large central pronotal spines; humerus triangular, with a large laterally produced spine in lateral apex of each side; two central pronotal spines and two humerus spines formed a transverse row in basal $^{2}/_{3}$ of posterior pronotal lobe; posterior margin of pronotum weakly concave, medially submerged; posterior angles round, slightly exceeding to posterior margin of pronotum (Fig. 12A). Scutellum roundly triangular, triangularly depressed basally, and sloping downward, posterior apex round (Fig. 12A). Femora elongated, slender but stout, moderate subnodulose apically, apical margin of femora with small spines evenly; tibiae slender and elongated. Hemelytra passing beyond apex of abdomen when fully closed, 0.7 times as long as body length (Fig. 11A); discal cell nearly diamond-shaped, slightly longer than wide (Fig. 12B); Sc 0.8 times as long as hemelytron length, 1.4 times as long as R+M (Fig. 12B). Hind wing about 3.6 times as long as maximum width (Fig. 12C). Laterotergites slightly dilated and ascending with segmental incisures, postero-lateral margin of each laterotergite not

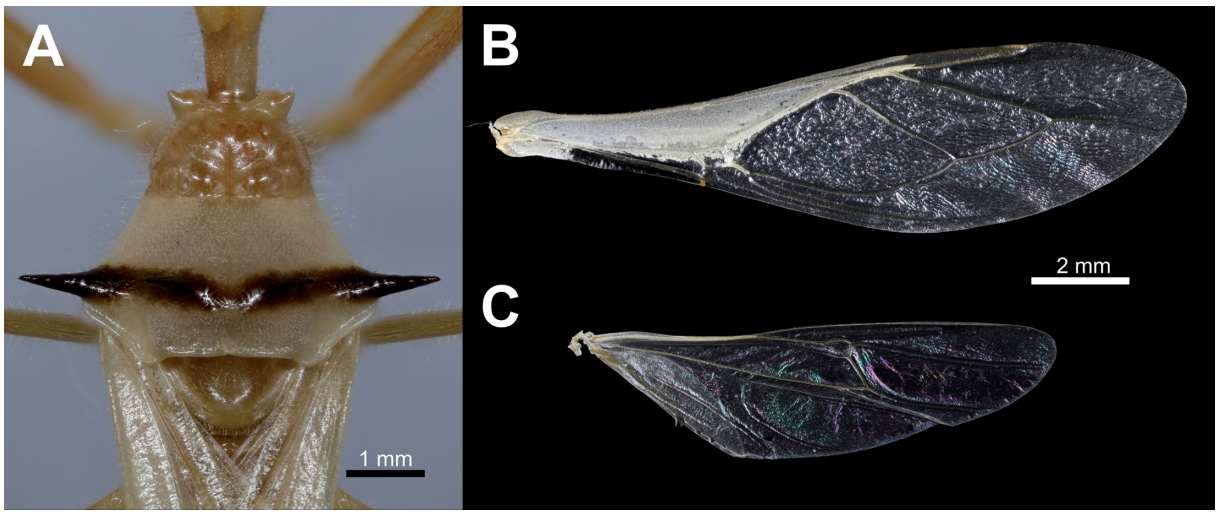

Fig. 12. *Epidaus konkakinhensis* Truong, Nguyen & Ha sp. nov., holotype, ♂ (TXL2022-148). **A**. Pronotum and scutellum in dorsal view. **B**. Right hemelytra. **C**. Right hind wing.

exceeding antero-lateral margin of following laterotergite (Fig. 11A–B). Pygophore ovoid (Fig. 13A–C); median process of pygophore (mpp) posteriorly produced, 0.48 times as long as wide in ventral view; apical margin reflexed, submerged medially and apicolateral corner specifically formed point at the apex, and separated to two large lateral thorns, each thorn with a smaller prickle nearly perpendicularly at base in caudal view (Fig. 13A–C); paramere long, slender, clavate, somewhat incurved in apical part, with round apex (Fig. 13A). Aedeagus in dorsal view ovoid, dorsally sclerotized, and in lateral view long and narrow (Fig. 13D–E); articulatory apparatus in ventral view with basal plate arms relatively slender and jointly forming a V-shape, and in lateral view arched strongly (Fig. 13D–E); dorsal phallothecal sclerite in lateral view with posteromedian weakly produced (Fig. 13E); spoon-like sclerites dissipated (Fig. 13D–E); membranous sac-like lobes almost disappeared (Fig. 13D–E); distal dorsal lobe of endosoma round and weakly bulged, without any thorns or prickles (Fig. 13D–E).

Vestiture. Body clothed with yellow setae. Head densely covered with short, slender, bent setae, interleaved with short, slender, erect setae; labium covered with short, slender, erect setae (Fig. 11C–D). Scape and pedicel covered with short, slender, sub-erect setae; remaining antennae covered with short, vertical setae,

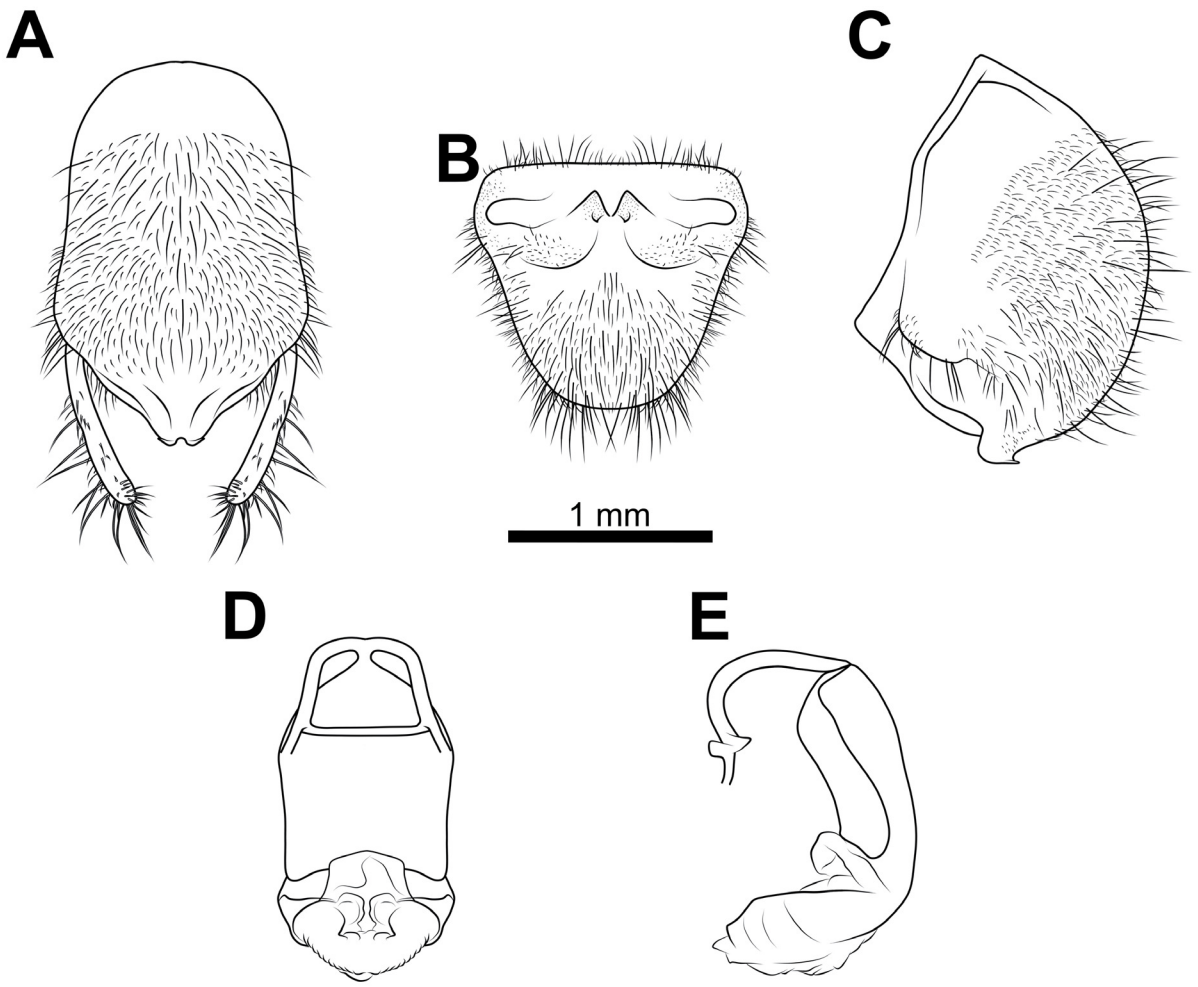

Fig. 13. *Epidaus konkakinhensis* Truong, Nguyen & Ha sp. nov., holotype, ♂ (TXL2022-148), genitalia. **A–C**. Pygophore. **A**. Pygophore with paramere in ventral view. **B**. Pygophore in caudal view. **C**. Pygophore in lateral view. **D–E**. Aedeagus with endosoma semi-everted. **D**. Dorsal view. **E**. Lateral view.

denser toward tip. Collar, anterolateral angles with tiny setae, somewhat interleaved with short, slender, erect setae; anterior pronotal lobe with some rows of tiny bent setae, somewhat interleave with slender, erect setae; posterior pronotal lobe covered densely with slender, erect setae; scutellum densely covered with short, slender, bent setae and interleaved with long slender erect setae (Fig. 12A). Coxae and trochanters covered with short, bent setae; femora, tibiae, and tarsi densely covered with long, slender, erect setae. Coria and clavus densely covered with short, bent setae. Abdominal mediotergites, laterotergites, and sternites covered with short, bent setae and slender, erect setae. Male genitalia pygophore ventrally and laterally densely covered with short and long setae (Fig. 13A–C); base of paramere almost glabrous, remaining part of paramere densely covered with short and long, thick, erect setae (Fig. 13A).

Measurements (all dimensions are given in mm)

Holotype (♂)

BL 20.49; HL 3.37; AoL 1.17; AoW 0.88; PoL 0.82; PoW 1.07; NL 0.77; OE 1.49; IE 0.67; ED 0.71; OD 0.19; OCD 0.52; COD 0.21; R1L 1.85; R2L 1.56; R3L 0.64; A1L 10.90; A2L 4.59; A3L 8.02; A4L 2.93; HSL 0.23; HSD 0.86; PnL 3.74; PnW 3.74; LPSD 5.36; APL 1.43; PPL 2.31; LPSL 1.06; CPSL 1.25; HeL 14.35; HeW 3.70; Sc 11.33; R+M 8.38; HWL 9.73; HWW 2.72; AFL 8.98; ATL 8.17; MFL 7.39; MTL 7.70; PFL 9.64; PTL 11.08.

Paratype (♂)

BL 19.16; HL 3.24; AoL 1.08; AoW 0.75; PoL 1.04; PoW 0.91; NL 0.59; OE 1.33; IE 0.67; ED 0.67; OD 0.18; OCD 0.49; COD 0.21; R1L 1.93; R2L 1.46; R3L 0.64; A1L 10.59; A2L 4.50; A3L 7.60; A4L 2.80; HSL 0.18; HSD 0.73; PnL 3.35; PnW 3.75; LPSD 5.12; APL 1.14; PPL 2.19; LPSL 1.04; CPSL 1.21; HeL 13.45; HeW 2.87; Sc 10.52; R+M 6.35; AFL 8.68; ATL 8.54; MFL 7.18; MTL 7.48; PFL 9.51; PTL 11.49.

Distribution

Vietnam (Gia Lai & Thua Thien Hue provinces).

Key to the Vietnamese species of genus Epidaus Stål, 1859

1. Four pronotal spines black or blackish brown, large and well produced 2
– Four pronotal spines black or brown, normal-sized and produced 4

2. Posterior pronotal lobe with black or blackish brown transverse band near posterior margin .... ***E. longispinus*** Hsiao, 1979
– Posterior pronotal lobe without black or blackish brown transverse band near posterior margin 3

3. Head reddish or brownish red .....***E. bachmaensis*** Truong, Zhao & Cai, 2006
– Head yellowish brown .....***E. batxatensis*** Truong, Nguyen & Ha sp. nov.
– Head pale orangish yellow ..... ***E. konkakinhensis*** Truong, Nguyen & Ha sp. nov.

4. Lateral and posterior area of pronotum, disk of scutellum, corium with small round white spots .... ***E. famulus*** (Stål, 1904)
– Lateral and posterior area of pronotum, disk of scutellum, corium without small round white spots ..... ***E. sexspinus*** Hsiao, 1979

Discussion

This study demonstrated that species discrimination of the Vietnamese species of *Epidaus* through conventional comparative morphological examination based on external and genital morphology of both male and female adults was consistent with the results of morphometric and molecular phylogenetic analyses. Through comparisons within the genus *Epidaus*, two new species, *Epidaus batxatensis* Truong,

Nguyen & Ha sp. nov., and *E. konkakinhensis* Truong, Nguyen & Ha sp. nov., were identified as distinct species using an integrative approach that combined morphological examination, morphometric analysis, and molecular phylogenetics.

Furthermore, the two newly described species, along with five previously named species, i.e., *Epidaus bachmaensis*, *E. famulus*, *E. insularis*, *E. longispinus*, and *E. wangi*, were successfully distinguished through PCA-based morphometric analyses. While further refinement of analytical methods and the inclusion of additional species of *Epidaus* would enhance the accuracy of species discrimination, our preliminary morphometric results suggest that this approach has significant potential. It serves as a valuable tool for distinguishing species and bridging molecular phylogeny-based classification with traditional morphology-based Linnaean taxonomy.

The utility of DNA-based phylogenetic and species delimitation analyses in the taxonomy of *Epidaus* and the broader Reduviidae family is now well established. However, most recognized species of *Epidaus* have been identified solely through morphological examination, and a comprehensive DNA barcode database for *Epidaus* remains largely unavailable. To address this gap, future studies should focus on collecting fresh or recently preserved specimens suitable for DNA sequencing to expand the genetic reference database and enhance taxonomic resolution.

Acknowledgments

The authors would like to thank Dr Le Hung Anh (Vice Director, Institute of Biology [IB], Vietnam Academy of Science and Technology, Vietnam), directors and staffs in Bat Xat Natural Reserve (Lao Cai Province) and Kon Ka Kinh National Park (Gia Lai Province), in Ta Leng and Then Sin, Tam Duong (Lai Chau Province) and Bach Ma National Park (Thua Thien Hue Province) for their kind assistance during our field activities. Moreover, we would like to send many thanks to our colleagues at IB and Vinh University, for their kind help and for sharing specimens. This research was funded by the Vietnam National Foundation for Science and Technology Development (NAFOSTED) under grant number 106.06-2021.38 to Truong Xuan Lam.

References

Ambrose D.P. 1999. *Assassin Bugs*. Science Publishers, Enfield, NH.

Bergroth E. 1915. Hemiptera from the Bombay Presidency. *Journal of Bombay Society* 24: 170–179.

Breddin G. 1900. Nova studia hemipterological. *Deutsche Entomologische Zeitschrift* 1: 161–185.

Burmeister H. 1835. *Handbuch der Entomologie*. *Tome 2*. G. Reimer, Berlin. https://doi.org/10.5962/bhl.title.8135

Chen Z., Zhu G., Wang J. & Cai W. 2016. *Epidaus wangi* (Hemiptera: Heteroptera: Reduviidae), a new assassin bug from Tibet, China. *Zootaxa* 4154 (1): 89–95. https://doi.org/10.11646/zootaxa.4154.1.6

Costa A. 1864. Generi e specie d'insetti della fauna Italian. *Annuario del Museo Zoologico della Università di Napoli* 2: 128–140. Available from https://www.biodiversitylibrary.org/page/11823222 [accessed 4 Aug. 2024].

Distant W.L. 1903. Rhynchotal notes. XVI. Heteroptera: Family Reduviidae (continued), Apiomerinae, Harpactorinae, and Nabinae. *Annals and Magazine of Natural History* 7 (11): 203–213, 245–258. https://doi.org/10.1080/00222930308678751

Distant W.L. 1904. *The Fauna of British India including Ceylon and Burma. Rhynchota. Volume II*. Taylor and Francis, London. https://doi.org/10.5962/bhl.title.48423

Distant W.L. 1919. The Heteroptera of Indo-China. *The Entomologist* 52: 207–211. Available from https://www.biodiversitylibrary.org/page/11935061 [accessed 4 Aug. 2024].

Forero D. & Weirauch C. 2012. Comparative genitalic morphology in the New World resin bugs Apiomerini (Hemiptera, Heteroptera, Reduviidae, Harpactorinae). *Deutsche Entomologische Zeitschrift* 59 (1): 5–41.

Ha N.L., Truong X.L., Ishikawa T., Jaitrong W., Lee C.F., Chouangthavy B. & Eguchi K. 2022. Three new species of the genus *Biasticus* Stål, 1867 (Insecta, Heteroptera, Reduviidae, Harpactorinae) from Central Highlands, Vietnam. *ZooKeys* 1118: 133–180. https://doi.org/10.3897/zookeys.1118.83156

Hajibabaei M., Janzen D.H., Burns J.M., Hallwachs W. & Hebert P.D.N. 2006. DNA barcodes distinguish species of tropical Lepidoptera. *Proceedings of the National Academy of Sciences USA* 103 (4): 968–971. https://doi.org/10.1073/pnas.0510466103

Hsiao T.Y. 1979. New species of Harpactorinae from China. I. (Hemiptera: Reduviidae). *Acta Zootaxonomica Sinica* 4: 137–155.

Hsiao T. & Ren S.Z. 1981. Hemiptera: Berytidae, Enicocephalidae, Reduviidae, Nabidae. *In*: *Insects of Xizang – Tibet. Vol. I.* Science Press, Beijing.

Jung S., Duwal R.K. & Lee S. 2011. COI barcoding of true bugs (Insecta, Heteroptera). *Molecular Ecology Resources* 11 (2): 266–270. https://doi.org/10.1111/j.1755-0998.2010.02945.x

Kalyaanamoorthy S., Minh B.Q., Wong T., von Haeseler A. & Jermiin L.S. 2017. ModelFinder: Fast model selection for accurate phylogenetic estimates. *Nature Methods* 14 (6): 587–589. https://doi.org/10.1038/nmeth.4285

Kassambara A. & Mundt F. 2020. Package 'factoextra': Extract and visualize the results of multivariate data analyses. Version 1.0.7. Available from https://cran.r-project.org/package=factoextra [accessed 4 Aug. 2024].

Khmelik V.V., Kozub D. & Glazunov A. 2006. Helicon Focus. Version 8.2.0 [Internet]. Helicon Soft Ltd., Ukraine. Available from https://www.heliconsoft.com/heliconfocus.html [accessed 4 Aug. 2024].

Kumar S., Stecher G., Li M., Knyaz C. & Tamura K. 2018. MEGA X: Molecular Evolutionary Genetics Analysis across computing platforms. *Molecular Biology and Evolution* 35 (6): 1547–1549. https://doi.org/10.1093/molbev/msy096

Larkin M.A., Blackshields G., Brown N.P., Chenna R., McGettigan P.A., McWilliam H., Miller, N.C.E. 1941. New genera and species of Malaysian Reduviidae (continued). Part II. *Journal of the Federated Malay States Museums* 18: 601–773.

Maldonado-Capriles J. 1990. *Systematic Catalogue of the Reduviidae of the World (Insecta: Heteroptera)*. A special edition of *Caribbean Journal of Science*, Puerto Rico.

Miller N.C.E. 1941. New genera and species of Malaysian Reduviidae (continued). Part II. *Journal of the Federated Malay States Museums* 18: 601–773.

Miller N.C.E. 1948. New genera and species of Reduviidae from the Philippines, Celebes, and Malaysia. *Transactions of the Entomological Society of London* 99 (13): 411–473. https://doi.org/10.1111/j.1365-2311.1948.tb01228.x

Miller N.C.E. 1956. *The Biology of the Heteroptera*. Leonard Hill Books, London.

Puillandre N., Brouillet S. & Achaz G. 2021. ASAP: Assemble Species by Automatic Partitioning. *Molecular Ecology Resources* 21 (2): 609–620. https://doi.org/10.1111/1755-0998.13281

Putshkov V.G. & Putshkov P.V. 1985. *A Catalogue of Assassin-bugs Genera of the World (Heteroptera, Reduviidae)*. VINITI, Moskva.

Putshkov V.G. & Putshkov P.V. 1996. Family Reduviidae Latreille, 1807 – Assassin-bugs. *In*: Aukema B. & Rieger C. (eds) *Catalogue of the Heteroptera of Palaearctic Region. Vol. 2*: 148–265. The Netherlands Entomological Society, Amsterdam.

R Core Team 2021. R: A Language and Environment for Statistical Computing. R Foundation for Statistical Computing, Vienna. Available from https://www.R-project.org [accessed 4 Aug. 2024].

Rambaut A., Drummond A.J., Xie D., Baele G. & Suchard M.A. 2018. Posterior summarisation in Bayesian phylogenetics using Tracer 1.7. *Systematic Biology* 67 (5): 901–904. https://doi.org/10.1093/sysbio/syy032

Ronquist F. & Huelsenbeck J.P. 2003. MrBayes: Bayesian phylogenetic inference under mixed models. *Bioinformatics* 19 (12): 1572–1574. https://doi.org/10.1093/bioinformatics/btg180

Rosa J.A., Mendonça V.J., Rocha C.S., Gardim S. & Cilense M. 2005. Characterization of the external female genitalia of six species of Triatominae (Hemiptera: Reduviidade) by scanning electron microscopy. *Memórias do Instituto Oswaldo Cruz, Rio de Janeiro* 105 (3): 286–292. https://doi.org/10.1590/S0074-02762010000300007

Satria R., Kurushima H., Herwina H., Yamane S. & Eguchi K. 2015. The trap-jaw ant genus *Odontomachus* Latreille from Sumatra, with a new species description. *Zootaxa* 4048 (1): 1–36. https://doi.org/10.11646/zootaxa.4048.1.1

Schuh R.T. & Weirauch C. 2020. *True Bugs of the World (Hemiptera: Heteroptera). Classification and Natural History. 2nd Edition.* Siri Scientific Press, Manchester.

Simon C., Frati F., Beckenbach A., Crespi B., Liu H. & Flook P. 1994. Evolution, weighting, and phylogenetic utility of mitochondrial gene sequences and a compilation of conserved polymerase chain reaction primers. *Annals of the Entomological Society of America* 87 (6): 651–701. https://doi.org/10.1093/aesa/87.6.651

Stål C. 1859. Till kannedomen om Reduvini. *Öfversigt of Kungliga Vetenskaps-Akademiens Förhandlingar* 16: 175–204. Available from https://www.biodiversitylibrary.org/page/15963297 [accessed 4 Aug. 2024)].

Stål C. 1863. Formae speciesque novae Reduviidum. *Annales de la Société entomologique de France* 4: 25–58. Available from https://www.biodiversitylibrary.org/page/8256963 [accessed 4 Aug. 2024].

Stål C. 1874. Enumeratio Reduviidarum Europae, Africae, Asiae, et Australiae. *In*: Enumeratio Hemipterorum, IV. *Kungliga Svenska Vetenskaps-Akademiens Handlingar* 12: 3–97. Available from https://www.biodiversitylibrary.org/page/41916867 [accessed 4 Aug. 2024].

Stöver B.C. & Müller K.F. 2010. TreeGraph 2: Combining and visualizing evidence from different phylogenetic analyses. *BMC Bioinformatics* 11 (7): 1–9. https://doi.org/10.1186/1471-2105-11-7

Truong X.L. 2019. *Study on Reduviids of Subfamily Harpactorinae (Heteroptera: Reduviidae) in Vietnam*. Science and Technics Publishing House, Hanoi.

Truong X.L., Zhao P. & Cai W. 2006. Taxonomic notes on the genus *Epidaus* Stål (Heteroptera: Reduviidae: Harpactorinae) from Vietnam, with the description of a new species. *Zootaxa* 1256 (1): 1–9. https://doi.org/10.11646/zootaxa.1256.1.1

Truong X.L., Phan T.G., Nguyen D.D., Tran P.M.C. & Ha N.L. 2024. Two new species of the genus *Sycanus* Amyot & Serville (Insecta: Hemiptera: Reduviidae: Harpactorinae) from Vietnam. *Zootaxa* 5481 (3): 301–325. https://doi.org/10.11646/zootaxa.5481.3.1

Yang H.S. 1940. A new species of Reduviidae (Heteroptera). *Bulletin of the Fan Memorial Institute of Biology: Zoology Series* 8: 105–108.

Zhang J., Kapli P., Pavlidis P. & Stamatakis A. 2013. A general species delimitation method with applications to phylogenetic placements. *Bioinformatics* 29 (22): 2869–2876. https://doi.org/10.1093/bioinformatics/btt499

Zhang W., Zhao P., Cao L. & Cai W. 2010. Description of a new species of genus *Epidaus* Stål (Hemiptera: Reduviidae: Harpactorinae) from China, with a key to Chinese species. *Zootaxa* 2517: 62–68. https://doi.org/10.11646/zootaxa.2517.1.7

Printed versions of all papers are deposited in the libraries of four of the institutes that are members of the *EJT* consortium: Muséum national d'Histoire naturelle, Paris, France; Meise Botanic Garden, Belgium; Royal Museum for Central Africa, Tervuren, Belgium; Royal Belgian Institute of Natural Sciences, Brussels, Belgium. The other members of the consortium are: Natural History Museum of Denmark, Copenhagen, Denmark; Naturalis Biodiversity Center, Leiden, the Netherlands; Museo Nacional de Ciencias Naturales-CSIC, Madrid, Spain; Leibniz Institute for the Analysis of Biodiversity Change, Bonn – Hamburg, Germany; National Museum of the Czech Republic, Prague, Czech Republic; The Steinhardt Museum of Natural History, Tel Aviv, Israël.

Supplementary material

Supp. file 1. Flowchart of morphometric analysis (Principal Component Analysis (PCA)). https://doi.org/10.5852/ejt.2025.1012.3037.13623

Supp. file 2. R_script_Epidaus_Morphometry.R. https://doi.org/10.5852/ejt.2025.1012.3037.13625

Supp. file 3. Measurement_Epidaus_male. https://doi.org/10.5852/ejt.2025.1012.3037.13627

Supp. file 4. Measurement_Epidaus_male_extended. https://doi.org/10.5852/ejt.2025.1012.3037.13629

Supp. file 5. Measurement_Epidaus_female. https://doi.org/10.5852/ejt.2025.1012.3037.13631

Supp. file 6. Morphological differences between the two new species and the previously known Vietnamese species of *Epidaus* Stål, 1859. https://doi.org/10.5852/ejt.2025.1012.3037.13633